

1 **A transcriptional regulatory atlas of coronavirus infection of**  
2 **human cells**

3 Scott A Ochsner & Neil J McKenna

4 The Signaling Pathways Project and Department of Molecular and  
5 Cellular Biology, Baylor College of Medicine, Houston, TX 77030

6 **Address Correspondence To:**

7 **Neil J. McKenna**

8 **Department of Molecular and Cellular Biology**

9 **Baylor College of Medicine**

10 **Houston, TX 77030**

11 **USA**

12 **e: [nmckenna@bcm.edu](mailto:nmckenna@bcm.edu)**

13 **t: 713-798-8568**

14

15 **Abstract**

16 Identifying transcriptional responses that are most consistently associated with  
17 experimental coronavirus (CoV) infection can help illuminate human cellular signaling  
18 pathways impacted by CoV infection. Here, we distilled over 3,000,000 data points from  
19 publically archived CoV infection transcriptomic datasets into consensus regulatory  
20 signatures, or consensomes, that rank genes based on their transcriptional  
21 responsiveness to infection of human cells by MERS, SARS-CoV-1 and SARS-CoV-2  
22 subtypes. We computed overlap between genes with elevated rankings in the CoV  
23 consensomes against those from transcriptomic and ChIP-Seq consensomes for nearly  
24 880 cellular signaling pathway nodes. Validating the CoV infection consensomes, we  
25 identified robust overlap between their highly ranked genes and high confidence targets  
26 of signaling pathway nodes with known roles in CoV infection. We then developed a  
27 series of use cases that illustrate the utility of the CoV consensomes for hypothesis  
28 generation around mechanistic aspects of the cellular response to CoV infection. We  
29 make the CoV infection datasets and their universe of underlying data points freely  
30 accessible through the Signaling Pathways Project web knowledgebase at  
31 <https://www.signalingpathways.org/datasets/index.jsf>.

32

## 33 **Introduction**

34 Infection by coronaviruses (CoV) represents a major current global public health  
35 concern. Signaling within and between airway epithelial and immune cells in response  
36 to infections by CoV and other viruses is coordinated by a complex network of signaling  
37 pathway nodes. These include chemokine and cytokine-activated receptors, signaling  
38 enzymes and transcription factors, and the genomic targets encoding their downstream  
39 effectors (Takeda et al., 2003; Stark et al., 1998; Darnell et al., 1994)]. We recently  
40 described the Signaling Pathways Project (SPP; (Ochsner et al., 2019), an integrated  
41 'omics knowledgebase designed to assist bench researchers in leveraging publically  
42 archived transcriptomic and ChIP-Seq datasets to generate research hypotheses. A  
43 unique aspect of SPP is its collection of consensus regulatory signatures, or  
44 consensomes, which rank genes based on the frequency of their significant differential  
45 expression across transcriptomic experiments mapped to a specific signaling pathway  
46 node or node family. By surveying across multiple independent datasets, we have  
47 shown that consensomes recapitulate pathway node-genomic target regulatory  
48 relationships to a high confidence level (Ochsner et al., 2019).

49 Placing the transcriptional events associated with human CoV infection in context with  
50 those associated with other signaling paradigms has the potential to catalyze the  
51 development of novel therapeutic approaches. The CoV research community has been  
52 active in generating and archiving transcriptomic datasets documenting the  
53 transcriptional response of human cells to infection by the three major CoV species,  
54 namely, Middle East respiratory syndrome coronavirus (MERS) and severe acute  
55 respiratory syndrome coronaviruses 1 (SARS1) and 2 (SARS2) (DeDiego et al., 2011;

56 Josset et al., 2013; Sims et al., 2013; Yoshikawa et al., 2010). To date however the field  
57 has lacked a resource that fully capitalizes on these datasets by, firstly, using them to  
58 rank human genes according to their transcriptional response to CoV infection and  
59 secondly, contextualizing these transcriptional responses by integrating them with  
60 'omics data points relevant to host cellular signaling pathways. Here, as a service to the  
61 research community to catalyze the development of novel CoV therapeutics, we  
62 generated consensomes for infection of human cells by MERS, SARS1 and SARS2  
63 CoVs. We then analyzed the extent to which high confidence transcriptional targets for  
64 these viruses intersected with genes with elevated rankings in transcriptomic and CHIP-  
65 Seq consensomes for cellular signaling pathway nodes. Integration of the CoV  
66 consensomes with the existing universes of SPP transcriptomic and CHIP-Seq data  
67 points in a series of use cases illuminates previously uncharacterized intersections  
68 between CoV infection and human cellular signaling pathways. The CoV infection  
69 consensome and its underlying datasets provide researchers with a unique and freely  
70 accessible framework within which to generate and pressure test hypotheses around  
71 human cellular signaling pathways impacted by CoV infection.

72

73

74

## 75 **Results**

### 76 **Generation of the CoV consensomes**

77 We first set out to generate a set of consensomes ranking human genes based on the  
78 frequency of their significant differential expression in response to infection by MERS,  
79 SARS1 and SARS2 CoVs. To do this we searched the Gene Expression Omnibus  
80 (GEO) and ArrayExpress databases to identify datasets involving infection of human  
81 cells by these species. From this initial collection of datasets, we next carried out a  
82 three step quality control check as previously described (Ochsner et al., 2019), yielding  
83 a total of 3,041,047 million data points in 111 experiments from 25 independent CoV  
84 infection transcriptomic datasets (Supplementary information, Section 1). Using these  
85 curated datasets, we next generated consensomes for each CoV species, as well as  
86 one ranking genes across all CoV infection experiments (ALL CoV). As a reference  
87 consensome for a virus whose transcriptional impact on human cells has been studied  
88 in depth, we also generated a consensome for human influenza A virus (IAV) infection.

89 The Supplementary information files contain the full human ALL CoV (Section 2), MERS  
90 (Section 3), SARS1 (Section 4), SARS2 (Section 5) and IAV (Section 6) infection  
91 transcriptomic consensomes. To assist researchers in inferring transcriptional regulation  
92 of signaling networks, the ALL CoV consensome is annotated to indicate the identity of  
93 a gene as encoding a bioactive small molecule, receptor, signaling enzyme or  
94 transcription factor (Supplementary information, Section 2, columns W-Z). As an initial  
95 benchmark for the ALL CoV consensome, we assembled a list of 20 interferon-  
96 stimulated genes (ISGs), which encode many of the key canonical viral response  
97 factors (Supplementary information, Section 2, column I) (Schneider et al., 2014). As

98 shown in the scatterplot representation of the ALL CoV consensome in Figure 1, all  
99 canonical ISGs were assigned appropriately elevated rankings in the consensome.

100 To gain insight into transcriptional intersections between CoV infection and human  
101 cellular signaling pathways, we next computed genes with elevated rankings in the CoV  
102 consensomes against genes with high confidence regulatory relationships with cellular  
103 signaling pathway nodes. To do this we generated five lists of genes corresponding to  
104 the ALL CoV, MERS, SARS1, SARS2 and IAV transcriptomic consensome 95<sup>th</sup>  
105 percentiles. We then retrieved genes in the 95<sup>th</sup> percentiles of human transcriptomic (n  
106 = 30) consensomes and ChIP-Seq (n = 834) consensomes for a collection of cellular  
107 signaling pathway nodes, and computed the extent and significance of their overlap with  
108 genes in the 95<sup>th</sup> percentiles of each of the five CoV consensomes. Significant overlap  
109 between the 95<sup>th</sup> percentiles of a node/node family consensome and a CoV  
110 consensome would indicate a potential biological relationship between loss or gain of  
111 function of that node and the transcriptional response to CoV infection.

112 For clarity and brevity we will refer from here on to the 95<sup>th</sup> percentile of a ChIP-Seq  
113 consensome as “CC95” and the 95<sup>th</sup> percentile of a transcriptomic consensome as  
114 “TC95”. Of the 834 node CC95s evaluated, 377 had significant overlap ( $p < 0.05$ ) with at  
115 least one of the CoV infection TC95s; of the 30 node/node family TC95s evaluated, 25  
116 had significant overlap ( $p < 0.05$ ) with at least one of the CoV infection TC95s. Results of  
117 these analyses are shown in Figure 2 (receptor and enzyme transcriptomic analysis),  
118 Figure 3 (ChIP-Seq transcription factor analysis), Figure 4 (ChIP-Seq enzyme analysis)  
119 and Figure 5 (ChIP-Seq co-node analysis); see also Supplementary information Section  
120 7 for the complete numerical data. We next surveyed the significant overlaps to identify

121 (i) canonical inflammatory signaling pathway nodes with characterized roles in the  
122 response to CoV infection, thereby validating the consensome approach in this context;  
123 and (ii) evidence for previously uncharacterized transcriptional biology of CoV infection  
124 that are consistent with their roles in the response to other viral infections.

125 **Receptors** Reflecting their well-documented roles in the response to viral infection, we  
126 observed appreciable significant overlap between all TC95s and those for the toll-like  
127 (TLR (Totura et al., 2015), interferon (IFNR (Hensley et al., 2004)) and tumor necrosis  
128 factor (TNFR (W. Wang et al., 2007)) receptor families (Fig. 2). Interestingly, these  
129 signatures were particularly highly enriched in the SARS2 TC95 – potentially reflecting a  
130 particularly strong antiviral response to infection by SARS2. TC95 overlaps for receptor  
131 systems with previously uncharacterized connections to CoV infection, including  
132 epidermal growth factor receptors, glucocorticoid receptor and NOTCH receptor  
133 signaling, are consistent with the known roles of these receptor systems in the context  
134 of other viral infections (Hayward, 2004; Ito et al., 2011; Ng et al., 2013; Ostler et al.,  
135 2019; Zheng et al., 2014). The relatively strong enrichment for xenobiotic receptors  
136 reflects work describing a role for pregnane X receptor in innate immunity (S. Wang et  
137 al., 2014) and points to a potential role for members of this family in the response to  
138 CoV infection.

139 **Transcription factors** In general, ChIP-Seq enrichments for transcription factors and  
140 other nodes were more specific for individual CoV infection TC95s (compare Fig. 2 with  
141 Figs 3, 4 and 5). This is likely due to the fact that ChIP-Seq consensomes are based on  
142 direct promoter binding by a specific node antigen, whereas transcriptomic  
143 consensomes encompass both direct and indirect targets of specific receptor and

144 enzyme node families. Not unexpectedly – and speaking again to validation of the  
145 consensomes - the strongest and most significant CoV TC95 overlaps were observed  
146 for CC95s for known transcription factor mediators of the transcriptional response to  
147 CoV infection, including members of the NFκB (Ludwig & Planz, 2008; Poppe et al.,  
148 2017; Ruckle et al., 2012), IRF (Chiang & Liu, 2018) and STAT (Blaszczyk et al., 2016;  
149 Frieman et al., 2007; Garcia-Sastre et al., 1998) transcription factor families. Consistent  
150 with its known role in the regulation of interferon-stimulated genes (Hasan et al., 2013),  
151 we also observed appreciable overlap between the CC95 for TFEB and the ALL CoV  
152 TC95. Moreover, the strong overlap between the GTF2B/TFIIB CC95 and all viral  
153 TC95s reflects previous evidence identifying GTF2B as a target for orthomyxovirus  
154 (Haas et al., 2018), herpes simplex virus (Gelev et al., 2014) and hepatitis B virus  
155 (Haviv et al., 1998).

156 **Enzymes** Compared to the roles of receptors and transcription factors in the response  
157 to viral infection, the roles of signaling enzymes are less well illuminated – indeed, in the  
158 context of CoV infection, they are entirely unstudied. Through their regulation of cell  
159 cycle transitions, cyclin-dependent kinases play important roles in the orchestration of  
160 DNA replication and cell division, processes that are critical in the viral life cycle. CDK6,  
161 which has been suggested to be a critical G1 phase kinase (Bellail et al., 2014; Grosse  
162 & Hinds, 2006), has been shown to be targeted by a number of viral infections, including  
163 Kaposi's sarcoma-associated herpesvirus (Kaldis et al., 2001) and HIV-1 (Pauls et al.,  
164 2014). Consistent with this common role across distinct viral infections, we observed  
165 robust overlap between the CDK95 TC95 (Fig. 2) and the CDK6 CC95 (Fig. 4) and  
166 those of all viral TC95s. As with the TLRs, IFNRs and TNFRs, which are known to



167 signal through CDK6 (Cingoz & Goff, 2018; Handschick et al., 2014; Hennessy et al.,  
168 2011), overlap with the CDK6 CC95 was particularly strong in the case of the SARS2  
169 TC95 (Fig. 4). CCNT2 is a member of the highly conserved family cyclin family and,  
170 along with CDK9, is a member of the viral-targeted p-TEFB complex (Zaborowska et al.,  
171 2016). Reflecting a potential general role in viral infection, appreciable overlap was  
172 observed between the CCNT2 CC95 and all viral TC95s (Fig. 4). Finally in the context  
173 of enzymes, DNA Topoisomerase (TOP1) has been shown to be required for efficient  
174 replication of simian virus 40 (Wobbe et al., 1987) and Ebola (Takahashi et al., 2013)  
175 viruses. The prominent overlap between its CC95 and those of SARS2 and IAV (Fig. 4)  
176 suggest that it may play a similar role in facilitating the replication of these viruses.

177 **Co-nodes** We have coined the term “co-nodes” as a convenient catch-all for cellular  
178 factors that are not members of the three principal signaling pathway node categories  
179 (receptors, enzymes and transcription factors; Ochsner et al., 2019). The breadth of  
180 functions encompassed by members of this category reflects the diverse mechanisms  
181 employed both by viruses to infect and propagate in cells, as well as by hosts to mount  
182 an efficient immune response. Consistent with its characterized role in the recruitment  
183 of p-TEFB by IV-1 Tat protein (Schulze-Gahmen et al., 2013), we observed consistently  
184 strong enrichment of the AFF4 CC95 in all viral TC95s (Fig. 5). The targeting of CNOT3  
185 for degradation in response to adenoviral infection (Chalabi Hagkarim et al., 2018) is  
186 reflected in the significant overlap between its CC95 and the viral TC95s, particularly in  
187 the case of the SARS2 (Fig. 5).

188 By way of additional independent validation of the CoV and IAV consensomes, Gene  
189 Set Enrichment Analysis (Subramanian et al., 2005) reflected significant overlap

190 between the CoV and IAV TC95s and a variety of viral infection and inflammatory  
191 transcription factor target gene sets (Supplementary information Section 8).

192

## 193 **Use cases**

194 Having established the reliability of the consensome approach in the context of CoV  
195 infection, we next wished to use the CoV consensomes to gather evidence to identify  
196 previously uncharacterized mediators of the transcriptional response to infection by  
197 CoVs and, of particular current interest, SARS2.

198

### 199 **Use case 1: consensome redundancy analysis identifies potential** 200 **uncharacterized players in the response to CoV infection**

201 We previously showed (Figs. 2 and 3) that the overlap of the CoV TC95 genes was  
202 most robust among consensomes for members of the IFNR, TLR and TNF receptor  
203 families (Fig. 2), and the NFkB, RELA, IRF and STAT transcription factor families (fig.  
204 5). To investigate this further, we ranked genes in the ALL CoV consensome by their  
205 aggregate 80<sup>th</sup> percentile rankings across these consensomes (Supplementary  
206 information, Section 2, column V). Transcriptomic consensomes for IFNRs (Section 9),  
207 TLRs (Section 10) and TNFRs (Section 11) are provided in Supplementary information,  
208 as are links to the ChIP-Atlas lists used to generate the ChIP-Seq consensomes  
209 (Section 12).

210 This redundancy ranking elevates genes with known critical roles in the response to  
211 viral infection that are acutely responsive to a spectrum of inflammatory signaling  
212 nodes, such as *NCOA7* (Doyle et al., 2018), *STAT* (Chapgier et al., 2009) and *TAP1*  
213 (Gruter et al., 1998). Interestingly, genes such as *PSMB9*, *CSRNP1* and *MRPL24* have  
214 ALL CoV discovery rates that are comparable to or exceed those of many of the classic  
215 viral response ISGs (Fig. 1), but are either largely or completely uncharacterized in the  
216 context of viral infection. This use case the reflects the potential of consensome-driven  
217 data mining to illuminate novel and potentially therapeutically relevant transcription  
218 pathway effectors in the response to CoV infection.

219

## 220 **Use case 2: discrimination between genes frequently differentially expressed in** 221 **response to CoV, but not IAV, infection**

222 We next wished to gain insight into signaling paradigms that were selectively  
223 characteristic of CoV infection but not IAV infection. To do this we generated a set of  
224 genes that were frequently differentially expressed in response to CoV infection (ALL  
225 CoV TC99), but less frequently expressed in response to IAV infection (50<sup>th</sup> percentile)  
226 (Table 1). Interestingly, this group contained two genes encoding transcription factors  
227 with well characterized roles in the regulation of oscillatory gene expression, *PER1* and  
228 *PER2* (Yamajuku et al., 2010). This led us to speculate that genomic targets of  
229 transcriptional regulators of circadian rhythms might be enriched among high  
230 confidence CoV-regulated genes, but not IAV-regulated genes. Consistent with this we  
231 observed significant overlap between the CC95s of the master circadian transcription  
232 factors ARNTL1/BMAL1 and CLOCK (Gaucher et al., 2018) and the CoV TC95, but not

233 the IAV TC95 (Fig. 2). These data indicate a hitherto uncharacterized intersection  
234 between CoV signaling and the cellular oscillatory apparatus. Another gene of note in  
235 this group is *INHBA*, encoding activin A, overexpression of which in murine lung gives  
236 rise to a phenotype resembling acute respiratory distress-like syndrome (Apostolou et  
237 al., 2012), a condition commonly associated with CoV infection (Totura & Bavari, 2019).  
238 Other genes in the group provide evidence for the potential mechanisms of infection  
239 and propagation of CoVs. *TJAP1*, for example, encodes a member of a family of  
240 proteins involved in regulation of tight junctions, shown to be route of porcine epidemic  
241 diarrhea coronavirus entry into epithelial cells (Luo et al., 2017). In addition, *GON7* is a  
242 member of the KEOPS complex (Wan et al., 2017), which is involved in  
243 threonylcarbamoylation of tRNAs, which represent an important host facet of the  
244 retroviral life cycle (Jin & Musier-Forsyth, 2019). Interestingly, another critical gene in  
245 this tRNA pathway, *YRDC*, is the 19<sup>th</sup> ranked gene in the ALL CoV consensome  
246 (Supplementary information Section 2).

247

### 248 **Use case 3: evidence for antagonism between progesterone receptor and** 249 **interferon receptor signaling in the airway epithelium**

250 Although a lack of clinical data has so far prevented a definitive evaluation of the  
251 connection between pregnancy and susceptibility to SARS2 infection in COVID-19,  
252 pregnancy has been previously associated with the incidence of viral infectious  
253 diseases, particularly respiratory infections (Sappenfield et al., 2013; Siston et al.,  
254 2010). We were interested therefore to see consistent overlap between the  
255 progesterone receptor (PGR) TC95 and all the viral TC95s, with the enrichment being

256 particularly evident in the case of the SARS2 TC95 (Fig. 2). To investigate the specific  
257 nature of the crosstalk implied by this overlap in the context of the airway epithelium, we  
258 first identified a set of 16 genes that were in both the ALL CoV and PGR TC95s. We  
259 then retrieved two SPP experiments involving treatment of A549 airway epithelial cells  
260 with the PGR full antagonist RU486 (RU), alone or in combination with the GR agonist  
261 dexamethasone (DEX). As shown in Figure 6 , there was nearly unanimous correlation  
262 in the direction of regulation of all 16 genes in response to CoV infection and PGR loss  
263 of function. These data indicate that antagonism between PGR and IFNR signaling in  
264 the airway epithelium may predispose pregnant women to infection by SARS2.

265

#### 266 **Use case 4: evidence for a role for the telomerase catalytic subunit TERT in the** 267 **interferon response to viral infection**

268 Although telomerase activation has been well characterized in the context of cell  
269 immortalization by human tumor virus infection (Gewin et al., 2004; Klingelhutz et al.,  
270 1996; Yang et al., 2004), no connection has previously been made between CoV or IAV  
271 infection and telomerase. We were therefore intrigued to observe robust overlap  
272 between all viral TC95s and that of the telomerase catalytic subunit TERT. In support of  
273 this finding, NFkB signaling has been shown to induce expression (Yin et al., 2000) and  
274 nuclear translocation (Akiyama et al., 2003) of TERT, and direct co-regulation by  
275 telomerase of NFkB-dependent transcription has been linked to chronic inflammation  
276 (Ghosh et al., 2012). Inspecting the ALL CoV consensome underlying data points (data  
277 not shown) we found that the *TERT* gene was not transcriptionally induced in response  
278 to infection by any of the CoVs, indicating that the overlap between its TC95 and those

279 of the CoVs might occur in response to an upstream regulatory signal. If functional  
280 interactions between TERT and inflammatory nodes did indeed take place in response  
281 to CoV infection, we anticipated that this would be reflected in close agreement  
282 regarding the direction of differential expression of CoV infection-regulated genes in  
283 response to perturbation of TERT on the one hand, and on the other, to stimulation of  
284 the classic viral response IFNRs. To test this hypothesis, we took the same set of 20  
285 ISGs referred to previously (Fig. 1) and compared their direction of regulation across all  
286 experiments underlying the ALL CoV, TERT and IFNR consensomes. For reference, the  
287 TERT consensome (Section 13) and its underlying data points (Section 14) are  
288 provided in the Supplementary information. With respect to the IFNR and TERT data  
289 points, we observed a nearly universal alignment in the direction of regulation of all  
290 genes tested with those in the CoV infection experiments (Fig. 6), with agreement in the  
291 direction of regulation across 99% of the underlying probesets. We should note that of  
292 the 1859  $p < 0.05$  CoV infection ISG data points, we observed repression, rather than  
293 induction, in response to CoV infection in 303 (~15%), which may be attributable to the  
294 impact of differences in cell type, cell cycle stage or virus incubation time across the  
295 independent experiments. Our results are consistent with a model in which activation of  
296 telomerase is a component of the human innate immune response to viral infection.

297

298 **Use case 5: SARS2 infection of human cells is specifically associated with an**  
299 **epithelial to mesenchymal transition transcriptional signature**

300 Epithelial to mesenchymal transition (EMT) is the process by which epithelial cells lose  
301 their polarity and adhesive properties and acquire the migratory and invasive

302 characteristics of mesenchymal stem cells (Lamouille et al., 2014). EMT is known to  
303 contribute to pulmonary fibrosis (Hill et al., 2019) and acute interstitial pneumonia (H. Li  
304 et al., 2014), both of which have been reported in connection with SARS2 infection in  
305 COVID-19 (Adair & Ledermann, 2020; P. Zhou et al., 2020). Moreover, EMT is widely  
306 accepted as a core component of the process by which renal tubular cells transform into  
307 mesenchymal cells during the development of fibrosis in kidney disease (Y. Liu, 2006),  
308 a signature comorbidity of SARS2 infection (Durvasula et al., 2020). Of the 834 CC95s  
309 analyzed, overlap ( $p < 0.05$ ) was specific to the SARS2 CC95 for only five; SNAI2/Slug,  
310 SOX2, GATA6, CTBP1 and PRMT1. Strikingly, a literature search indicated that these  
311 five nodes were connected by documented roles in in the promotion of EMT (Avasarala  
312 et al., 2015; Herreros-Villanueva et al., 2013; Martinelli et al., 2017; Nieto, 2002; Sahu  
313 et al., 2017). In addition to these nodes, whose C95 genes were exclusively enriched ( $p$   
314  $< 0.05$ ) in the SARS2 C95 genes, we identified several other EMT-linked nodes whose  
315 CC95 genes were preferentially enriched ( $p < 0.05$ ) in the SARS2 TC95 genes (Figs. 3-  
316 5), including the homeodomain transcription factor SIX2 (C.-A. Wang et al., 2014),  
317 SMAD4 (Siraj et al., 2019), and the co-nodes PYGO2 (Chi et al., 2019), SKI (Tecalco-  
318 Cruz et al., 2018), BRD7 (T. Liu et al., 2017) and STAG2 (Nie et al., 2019).

319 To investigate this further, we computed overlap between the individual viral TC99s and  
320 a list of 335 genes manually curated from the research literature as signature EMT  
321 markers (Supplementary information Section 15; Zhao et al., 2015). Consistent with the  
322 node consensome enrichment analysis, we observed significant enrichment of  
323 members of this gene set within the SARS2 CC99, but not those of the ALL CoV,  
324 SARS1, MERS or IAV consensomes (Supplementary information Section 16). One

325 possible explanation for this was the fact that the SARS2 consensome was comprised  
326 of airway epithelial cell lines, whereas the SARS1 and MERS consensomes included  
327 non-epithelial cell biosamples (Supplementary information Section 1). To exclude this  
328 possibility therefore, we next calculated airway epithelial cell-specific consensomes for  
329 SARS1 and MERS and computed overlap of their TC95s against the 864 pathway  
330 node/node family CC95s & TC95s. We found that significant overlap with the CoV  
331 TC95s remained specific to SARS2 (data not shown), confirming that significant overlap  
332 with the EMT node signature was specific to the SARS2 TC99.

333 We next applied consensome redundancy analysis (see Use case 1) to isolate a set of  
334 SARS2 regulated genes (CPV  $P < 0.05$ ) that were high confidence targets (i.e. in the  
335 CC80) for at least two of the EMT nodes (SNAI2, SOX2, GATA6, CTBP1 and PRMT1;  
336 Supplementary information, Section 4, column M). A literature survey showed that 13 of  
337 these 21 genes had a documented connection to EMT (Supplementary information,  
338 Section 5, column N). Figure 9 compares the percentile rankings for these genes across  
339 the three CoV infection consensomes and the IAV consensome. Although some EMT  
340 genes, such as *CXCL2* and *IRF9*, had elevated rankings across all four consensomes,  
341 the collective EMT gene signature had a significantly higher mean percentile value in  
342 the SARS2 consensome than in each of the three others (Fig. 9).

343 Although EMT has been associated with infection by transmissible gastroenteritis virus  
344 (Xia et al., 2017), this is to our knowledge the first evidence connecting CoV infection,  
345 and specifically SARS2 infection, to EMT. Interestingly, several members of the group  
346 of SARS2-induced EMT genes have been associated with signature pulmonary  
347 comorbidities of CoV infection, including ADAR (Diaz-Pina et al., 2018), CLDN1



348 (Vukmirovic et al., 2017) and SOD2 (Gao et al., 2008). Of note in the context of these  
349 data is the fact that signaling through two SARS2 cellular receptors, ACE2/AT2 and  
350 CD147/basigin, has been linked to EMT in the context of organ fibrosis (Kato et al.,  
351 2011; Ruster & Wolf, 2011; C. Wang et al., 2018). Moreover, overlap between of the  
352 CoV TC95s and the TERT CC95 was particularly robust in the case of SARS2, a finding  
353 of potential relevance to the fact that telomerase has been implicated in EMT (Z. Liu et  
354 al., 2013). Collectively, our data indicate that EMT warrants further investigation as a  
355 SARS2-specific pathological mechanism.

### 356 **Development of a CoV infection cell signaling knowledgebase**

357 Having validated the ALL CoV consensome, we next wished to make it freely available  
358 to the research community for re-use in the characterization of signaling events  
359 associated with CoV infection. Firstly, the viral infection datasets were curated  
360 accordingly to our previously described protocol (Ochsner et al., 2019) made available  
361 for browsing in the SPP Dataset listing  
362 (<https://www.signalingpathways.org/datasets/index.jsf>). As with other SPP datasets, and  
363 per FAIR data best practice, CoV infection datasets were associated with detailed  
364 descriptions, assigned a digital object identifier, and linked to the associated article to  
365 place the dataset in its original experimental context. Loading the CoV datasets into the  
366 SPP also automatically made the underlying data points discoverable by the SPP query  
367 tool Ominer (Ochsner et al., 2019). These reports represent a summary of the current  
368 state of transcriptomic and ChIP-Seq knowledge on the regulatory relationship of a  
369 given gene with upstream regulatory pathway nodes, or in clinical and model  
370 experiments. The full value of the integration of the CoV consensome with the existing

371 SPP framework can perhaps be best appreciated in the context of the one click links to  
372 Ominer Regulation Reports from the individual CoV datasets. These Reports provide  
373 researchers with a wealth of contextual data on signaling pathways impacted by CoV  
374 infection in the context of a specific gene. Table 2 shows links to Regulation Reports for  
375 the top twenty ranked genes in the ALL CoV consensome. The order of sections in the  
376 Reports is Receptors, Enzymes, Transcription Factors, Co-nodes, Clinical and Models,  
377 the last section including data points from the CoV infection model experiments that  
378 form the basis of this study.

## 379 Discussion

380 An effective research community response to the impact of CoVs on human health  
381 demands systematic exploration of the transcriptional interface between viral infection  
382 and human cell signaling systems. It also demands routine access to existing datasets  
383 that is unhindered either by paywalls or by lack of the informatics training required to  
384 manipulate archived datasets in their unprocessed state. Moreover, the substantial  
385 logistical obstacles to BSL3 certification only emphasizes the need for fullest possible  
386 access to, and re-usability of, existing CoV infection datasets to focus and refine  
387 hypotheses prior to carrying out *in vivo* CoV infection experiments. To this end, we  
388 generated a set of CoV infection consensomes that rank human genes by the  
389 reproducibility of their significant differential expression in response to infection of  
390 human cells by CoVs. We then computed the CoV consensomes against high  
391 confidence transcriptional signatures for a broad range of cellular signaling pathway  
392 nodes, affording investigators with a broad range of signaling interests an entrez into  
393 the study of CoV infection of human cells. The five use cases described here represent  
394 illustrative examples of the types of analyses that users are empowered to carry out in  
395 the CoV infection knowledgebase.

396 To democratize access to the CoV consensome and its >3,000,000 underlying data  
397 points by the broadest possible audience, we have integrated them into the SPP  
398 database to create a cell signaling knowledgebase for CoV infection. Incorporation of  
399 the CoV data points into SPP in this manner places them in the context of millions more  
400 existing SPP data points documenting transcriptional regulatory relationships between  
401 pathway nodes and their genomic targets. In doing so, we afford users a unique

402 appreciation of the cellular signaling pathway nodes whose gain or loss of function in  
403 response to CoV infection gives rise to these transcriptional patterns.

404 The human CoV and IAV consensomes and their underlying datasets are “living”  
405 resources on SPP that will be updated and versioned with appropriate datasets. This  
406 will be particularly important in the case of SARS2, as datasets involving infection of  
407 human cells with this virus are necessarily currently limited in number. This will allow  
408 for hardening of observations that are intriguing, but whose significance is currently  
409 unclear, such as the overlap of the CoV TC95s with the TERT TC95, as well as the  
410 enrichment of EMT genes among those with elevated rankings in the SARS2  
411 consensome. We welcome feedback and suggestions from the research community for  
412 the future development of the SPP CoV infection consensomes.

413

414

415

416

417

## 418 **Methods**

### 419 **Dataset processing and consensome analysis.**

420 Differential expression values were calculated for each gene in each experiment using  
421 the limma analysis package from Bioconductor then committed to the consensome  
422 analysis pipeline as previously described (Ochsner et al., 2019). Briefly, the  
423 consensome algorithm surveys each experiment across all datasets and ranks genes  
424 according to the frequency with which they are significantly differentially expressed. For  
425 each transcript, we counted the number of experiments where the significance for  
426 differential expression was  $\leq 0.05$ , and then generated the binomial probability, referred  
427 to as the consensome p-value (CPV), of observing that many or more nominally  
428 significant experiments out of the number of experiments in which the transcript was  
429 assayed, given a true probability of 0.05. A more detailed description of the  
430 transcriptomic consensome algorithm is available (Ochsner et al., 2019). The  
431 consensomes and underlying datasets were loaded into an Oracle 13c database and  
432 made available on the SPP user interface as previously described (Ochsner et al.,  
433 2019).

### 434 **Statistical analysis**

435 Gene Overlap analysis was performed using the Bioconductor GeneOverlap analysis  
436 package  
437 (<https://www.rdocumentation.org/packages/GeneOverlap/versions/1.8.0/topics/GeneOverlap>)  
438 implemented in R. Briefly, given a whole set  $I$  of IDs and two sets  $A \in I$  and  $B \in I$ ,  
439 and  $S = A \cap B$ , GeneOverlap calculates the significance of obtaining  $S$ . The problem is

440 formulated as a hypergeometric distribution or a contingency table, which is solved by  
441 Fisher's exact test. The universe for the overlap was set at a recent estimate of the total  
442 number of coding genes in the human genome (21,500; Pertea et al., 2018). Paired  
443 Two Sample t-Test for comparing the mean percentile ranking of EMT genes in the  
444 MERS, SARS1, SARS2 and IAV consensomes was performed in PRISM at 12 degrees  
445 of freedom.

#### 446 **Consensome generation**

447 The procedure for generating transcriptomic consensomes has been previously  
448 described (Ochsner et al., 2019). To generate the CHIP-Seq consensomes, we first  
449 retrieved processed gene lists from CHIP-Atlas, which rank human genes based upon  
450 their average MACS2 occupancy across all publically archived datasets in which a  
451 given transcription factor, enzyme or co-node is the IP antigen. Of the three stringency  
452 levels available (10, 5 and 1 kb from the transcription start site), we selected the most  
453 stringent (1 kb). According to SPP convention (Ochsner et al., 2019), we then mapped  
454 the IP antigen to its pathway node category and class, and the experimental cell line to  
455 its appropriate biosample physiological system and organ. We then organized the  
456 ranked lists into percentiles to generate the node CHIP-Seq consensome.

#### 457 **SPP web application**

458 The SPP knowledgebase is a gene-centric Java Enterprise Edition 6, web-based  
459 application around which other gene, mRNA, protein and BSM data from external  
460 databases such as NCBI are collected. After undergoing semiautomated processing  
461 and biocuration as described above, the data and annotations are stored in SPP's

462 Oracle 13c database. RESTful web services exposing SPP data, which are served to  
463 responsively designed views in the user interface, were created using a Flat UI Toolkit  
464 with a combination of JavaScript, D3.JS, AJAX, HTML5, and CSS3. JavaServer Faces  
465 and PrimeFaces are the primary technologies behind the user interface. SPP has been  
466 optimized for Firefox 24+, Chrome 30+, Safari 5.1.9+, and Internet Explorer 9+, with  
467 validations performed in BrowserStack and load testing in LoadUIWeb. XML describing  
468 each dataset and experiment is generated and submitted to CrossRef to mint DOIs  
469 (Ochsner et al., 2019).

470

## 471 **Data availability**

472 The entire set of data points used to generate the CoV consensome has been uploaded in an R  
473 file to Figshare and a link included for reviewer access. The entire set of metadata for these  
474 data points is available in Supplementary information Section 1. Consensome data points are in  
475 Supplementary information Sections 2-6.

476 SPP is freely accessible at <https://www.signalingpathways.org>. Programmatic access to all  
477 underlying data points and their associated metadata are supported by a RESTful API at  
478 <https://www.signalingpathways.org/docs/>. All SPP datasets are biocurated versions of publically  
479 archived datasets, are formatted according to the recommendations of the FORCE11 Joint  
480 Declaration on Data Citation Principles<sup>74</sup>, and are made available under a Creative Commons  
481 CC 3.0 BY license. The original datasets are available are linked to from the corresponding SPP  
482 datasets using the original repository accession identifiers. These identifiers are for  
483 transcriptomic datasets, the Gene Expression Omnibus (GEO) Series (GSE); and for  
484 cistromic/ChIP-Seq datasets, the NCBI Sequence Read Archive (SRA) study identifier (SRP).  
485 DOIs for the consensomes and datasets are pending.

## 486 **Code availability**

487 The full SPP source code is available in the SPP GitHub account under a Creative Commons  
488 CC 3.0 BY license at <https://github.com/signaling-pathways-project/ominer/>.



## 489 **Acknowledgements**

490 This work was supported by the National Institute of Diabetes, Digestive and Kidney  
491 Diseases NIDDK Information Network U24 (DK097748), the National Cancer Institute  
492 (CA125123) and by the Brockman Medical Research Foundation. We appreciate the  
493 technical assistance of Apollo McOwiti and Shijing Qu of the Biostatistics and  
494 Informatics Shared Resource of the Duncan NCI Comprehensive Cancer Center. We  
495 thank all investigators who archive their datasets, without whom SPP would not be  
496 possible.

497

## 498 **Author contributions**

499 **Dataset biocuration:** SO

500 **Data analysis:** SO, NM

501 **Manuscript drafting:** NM

502

## 503 **Competing interests**

504 The authors declare no competing interests.

505

506

## 507 **References**

- 508 Adair, L. B. 2nd, & Ledermann, E. J. (2020). Chest CT Findings of Early and  
509 Progressive Phase COVID-19 Infection from a US Patient. In *Radiology case*  
510 *reports*. <https://doi.org/10.1016/j.radcr.2020.04.031>
- 511 Akiyama, M., Hideshima, T., Hayashi, T., Tai, Y.-T., Mitsiades, C. S., Mitsiades, N.,  
512 Chauhan, D., Richardson, P., Munshi, N. C., & Anderson, K. C. (2003). Nuclear  
513 factor-kappaB p65 mediates tumor necrosis factor alpha-induced nuclear  
514 translocation of telomerase reverse transcriptase protein. *Cancer Research*, *63*(1),  
515 18–21.
- 516 Apostolou, E., Stavropoulos, A., Sountoulidis, A., Xirakia, C., Giaglis, S.,  
517 Protopapadakis, E., Ritis, K., Mentzelopoulos, S., Pasternack, A., Foster, M.,  
518 Ritvos, O., Tzelepis, G. E., Andreakos, E., & Sideras, P. (2012). Activin-A  
519 overexpression in the murine lung causes pathology that simulates acute  
520 respiratory distress syndrome. *American Journal of Respiratory and Critical Care*  
521 *Medicine*, *185*(4), 382–391. <https://doi.org/10.1164/rccm.201105-0784OC>
- 522 Avasarala, S., Van Scoyk, M., Karuppusamy Rathinam, M. K., Zerayesus, S., Zhao, X.,  
523 Zhang, W., Pergande, M. R., Borgia, J. A., DeGregori, J., Port, J. D., Winn, R. A., &  
524 Bikkavilli, R. K. (2015). PRMT1 Is a Novel Regulator of Epithelial-Mesenchymal-  
525 Transition in Non-small Cell Lung Cancer. *The Journal of Biological Chemistry*,  
526 *290*(21), 13479–13489. <https://doi.org/10.1074/jbc.M114.636050>
- 527 Barata, J. T., Durum, S. K., & Seddon, B. (2019). Flip the coin: IL-7 and IL-7R in health  
528 and disease. *Nature Immunology*, *20*(12), 1584–1593.  
529 <https://doi.org/10.1038/s41590-019-0479-x>
- 530 Bellail, A. C., Olson, J. J., & Hao, C. (2014). SUMO1 modification stabilizes CDK6  
531 protein and drives the cell cycle and glioblastoma progression. *Nature*  
532 *Communications*, *5*, 4234. <https://doi.org/10.1038/ncomms5234>
- 533 Blaszczyk, K., Nowicka, H., Kostyrko, K., Antonczyk, A., Wesoly, J., & Bluysen, H. A.  
534 R. (2016). The unique role of STAT2 in constitutive and IFN-induced transcription  
535 and antiviral responses. *Cytokine & Growth Factor Reviews*, *29*, 71–81.  
536 <https://doi.org/10.1016/j.cytogfr.2016.02.010>
- 537 Chalabi Hagkarim, N., Ryan, E. L., Byrd, P. J., Hollingworth, R., Shimwell, N. J.,  
538 Agathangelou, A., Vavasseur, M., Kolbe, V., Speiseder, T., Dobner, T., Stewart,  
539 G. S., & Grand, R. J. (2018). Degradation of a Novel DNA Damage Response  
540 Protein, Tankyrase 1 Binding Protein 1, following Adenovirus Infection. *Journal of*  
541 *Virology*, *92*(12). <https://doi.org/10.1128/JVI.02034-17>
- 542 Chang, B., Yang, H., Jiao, Y., Wang, K., Liu, Z., Wu, P., Li, S., & Wang, A. (2016).  
543 SOD2 deregulation enhances migration, invasion and has poor prognosis in  
544 salivary adenoid cystic carcinoma. *Scientific Reports*, *6*, 25918.  
545 <https://doi.org/10.1038/srep25918>

- 546 Chappier, A., Kong, X.-F., Boisson-Dupuis, S., Jouanguy, E., Averbuch, D., Feinberg,  
547 J., Zhang, S.-Y., Bustamante, J., Vogt, G., Lejeune, J., Mayola, E., de  
548 Beaucoudrey, L., Abel, L., Engelhard, D., & Casanova, J.-L. (2009). A partial form  
549 of recessive STAT1 deficiency in humans. *The Journal of Clinical Investigation*,  
550 119(6), 1502–1514. <https://doi.org/10.1172/JCI37083>
- 551 Chi, Y., Wang, F., Zhang, T., Xu, H., Zhang, Y., Shan, Z., Wu, S., Fan, Q., & Sun, Y.  
552 (2019). miR-516a-3p inhibits breast cancer cell growth and EMT by blocking the  
553 Pygo2/Wnt signalling pathway. *Journal of Cellular and Molecular Medicine*, 23(9),  
554 6295–6307. <https://doi.org/10.1111/jcmm.14515>
- 555 Chiang, H.-S., & Liu, H. M. (2018). The Molecular Basis of Viral Inhibition of IRF- and  
556 STAT-Dependent Immune Responses. *Frontiers in Immunology*, 9, 3086.  
557 <https://doi.org/10.3389/fimmu.2018.03086>
- 558 Cingoz, O., & Goff, S. P. (2018). Cyclin-dependent kinase activity is required for type I  
559 interferon production. *Proceedings of the National Academy of Sciences of the*  
560 *United States of America*, 115(13), E2950–E2959.  
561 <https://doi.org/10.1073/pnas.1720431115>
- 562 Darnell, J. E. J., Kerr, I. M., & Stark, G. R. (1994). Jak-STAT pathways and  
563 transcriptional activation in response to IFNs and other extracellular signaling  
564 proteins. *Science (New York, N.Y.)*, 264(5164), 1415–1421.  
565 <https://doi.org/10.1126/science.8197455>
- 566 DeDiego, M. L., Nieto-Torres, J. L., Jimenez-Guardeno, J. M., Regla-Nava, J. A.,  
567 Alvarez, E., Oliveros, J. C., Zhao, J., Fett, C., Perlman, S., & Enjuanes, L. (2011).  
568 Severe acute respiratory syndrome coronavirus envelope protein regulates cell  
569 stress response and apoptosis. *PLoS Pathogens*, 7(10), e1002315.  
570 <https://doi.org/10.1371/journal.ppat.1002315>
- 571 Diaz-Pina, G., Ordonez-Razo, R. M., Montes, E., Paramo, I., Becerril, C., Salgado, A.,  
572 Santibanez-Salgado, J. A., Maldonado, M., & Ruiz, V. (2018). The Role of ADAR1  
573 and ADAR2 in the Regulation of miRNA-21 in Idiopathic Pulmonary Fibrosis. *Lung*,  
574 196(4), 393–400. <https://doi.org/10.1007/s00408-018-0115-9>
- 575 Doherty, M. R., Cheon, H., Junk, D. J., Vinayak, S., Varadan, V., Telli, M. L., Ford, J.  
576 M., Stark, G. R., & Jackson, M. W. (2017). Interferon-beta represses cancer stem  
577 cell properties in triple-negative breast cancer. *Proceedings of the National*  
578 *Academy of Sciences of the United States of America*, 114(52), 13792–13797.  
579 <https://doi.org/10.1073/pnas.1713728114>
- 580 Doyle, T., Moncorge, O., Bonaventure, B., Pollpeter, D., Lussignol, M., Tauziet, M.,  
581 Apolonia, L., Catanese, M.-T., Goujon, C., & Malim, M. H. (2018). The interferon-  
582 inducible isoform of NCOA7 inhibits endosome-mediated viral entry. *Nature*  
583 *Microbiology*, 3(12), 1369–1376. <https://doi.org/10.1038/s41564-018-0273-9>
- 584 Durvasula, R., Wellington, T., McNamara, E., & Watnick, S. (2020). COVID-19 and  
585 Kidney Failure in the Acute Care Setting: Our Experience From Seattle. In

- 586 *American journal of kidney diseases : the official journal of the National Kidney*  
587 *Foundation*. <https://doi.org/10.1053/j.ajkd.2020.04.001>
- 588 Ercolano, G., De Cicco, P., Rubino, V., Terrazzano, G., Ruggiero, G., Carriero, R.,  
589 Kunderfranco, P., & Ianaro, A. (2019). Knockdown of PTGS2 by CRISPR/CAS9  
590 System Designates a New Potential Gene Target for Melanoma Treatment.  
591 *Frontiers in Pharmacology*, *10*, 1456. <https://doi.org/10.3389/fphar.2019.01456>
- 592 Frieman, M., Yount, B., Heise, M., Kopecky-Bromberg, S. A., Palese, P., & Baric, R. S.  
593 (2007). Severe acute respiratory syndrome coronavirus ORF6 antagonizes STAT1  
594 function by sequestering nuclear import factors on the rough endoplasmic  
595 reticulum/Golgi membrane. *Journal of Virology*, *81*(18), 9812–9824.  
596 <https://doi.org/10.1128/JVI.01012-07>
- 597 Gao, F., Kinnula, V. L., Myllarniemi, M., & Oury, T. D. (2008). Extracellular superoxide  
598 dismutase in pulmonary fibrosis. *Antioxidants & Redox Signaling*, *10*(2), 343–354.  
599 <https://doi.org/10.1089/ars.2007.1908>
- 600 Garcia-Sastre, A., Durbin, R. K., Zheng, H., Palese, P., Gertner, R., Levy, D. E., &  
601 Durbin, J. E. (1998). The role of interferon in influenza virus tissue tropism. *Journal*  
602 *of Virology*, *72*(11), 8550–8558.
- 603 Gaucher, J., Montellier, E., & Sassone-Corsi, P. (2018). Molecular Cogs: Interplay  
604 between Circadian Clock and Cell Cycle. *Trends in Cell Biology*, *28*(5), 368–379.  
605 <https://doi.org/10.1016/j.tcb.2018.01.006>
- 606 Gelev, V., Zabolotny, J. M., Lange, M., Hiromura, M., Yoo, S. W., Orlando, J. S.,  
607 Kushnir, A., Horikoshi, N., Paquet, E., Bachvarov, D., Schaffer, P. A., & Usheva, A.  
608 (2014). A new paradigm for transcription factor TFIIB functionality. *Scientific*  
609 *Reports*, *4*, 3664. <https://doi.org/10.1038/srep03664>
- 610 Gewin, L., Myers, H., Kiyono, T., & Galloway, D. A. (2004). Identification of a novel  
611 telomerase repressor that interacts with the human papillomavirus type-16 E6/E6-  
612 AP complex. *Genes & Development*, *18*(18), 2269–2282.  
613 <https://doi.org/10.1101/gad.1214704>
- 614 Ghosh, A., Saginc, G., Leow, S. C., Khattar, E., Shin, E. M., Yan, T. D., Wong, M.,  
615 Zhang, Z., Li, G., Sung, W.-K., Zhou, J., Chng, W. J., Li, S., Liu, E., & Tergaonkar,  
616 V. (2012). Telomerase directly regulates NF-kappaB-dependent transcription.  
617 *Nature Cell Biology*, *14*(12), 1270–1281. <https://doi.org/10.1038/ncb2621>
- 618 Gressel, M. J., & Hinds, P. W. (2006). Beyond the cell cycle: a new role for Cdk6 in  
619 differentiation. *Journal of Cellular Biochemistry*, *97*(3), 485–493.  
620 <https://doi.org/10.1002/jcb.20712>
- 621 Gruter, P., Tabernero, C., von Kobbe, C., Schmitt, C., Saavedra, C., Bachi, A., Wilm,  
622 M., Felber, B. K., & Izaurralde, E. (1998). TAP, the human homolog of Mex67p,  
623 mediates CTE-dependent RNA export from the nucleus. *Molecular Cell*, *1*(5), 649–  
624 659. [https://doi.org/10.1016/s1097-2765\(00\)80065-9](https://doi.org/10.1016/s1097-2765(00)80065-9)

- 625 Haas, D. A., Meiler, A., Geiger, K., Vogt, C., Preuss, E., Kochs, G., & Pichlmair, A.  
626 (2018). Viral targeting of TFIIIB impairs de novo polymerase II recruitment and  
627 affects antiviral immunity. *PLoS Pathogens*, 14(4), e1006980.  
628 <https://doi.org/10.1371/journal.ppat.1006980>
- 629 Handschick, K., Beuerlein, K., Jurida, L., Bartkuhn, M., Muller, H., Soelch, J., Weber, A.,  
630 Dittrich-Breiholz, O., Schneider, H., Scharfe, M., Jarek, M., Stellzig, J., Schmitz, M.  
631 L., & Kracht, M. (2014). Cyclin-dependent kinase 6 is a chromatin-bound cofactor  
632 for NF-kappaB-dependent gene expression. *Molecular Cell*, 53(2), 193–208.  
633 <https://doi.org/10.1016/j.molcel.2013.12.002>
- 634 Hasan, M., Koch, J., Rakheja, D., Pattnaik, A. K., Brugarolas, J., Dozmorov, I., Levine,  
635 B., Wakeland, E. K., Lee-Kirsch, M. A., & Yan, N. (2013). Trex1 regulates  
636 lysosomal biogenesis and interferon-independent activation of antiviral genes.  
637 *Nature Immunology*, 14(1), 61–71. <https://doi.org/10.1038/ni.2475>
- 638 Haviv, I., Shamay, M., Doitsh, G., & Shaul, Y. (1998). Hepatitis B virus pX targets TFIIIB  
639 in transcription coactivation. *Molecular and Cellular Biology*, 18(3), 1562–1569.  
640 <https://doi.org/10.1128/mcb.18.3.1562>
- 641 Hayward, S. D. (2004). Viral interactions with the Notch pathway. *Seminars in Cancer*  
642 *Biology*, 14(5), 387–396. <https://doi.org/10.1016/j.semcancer.2004.04.018>
- 643 Hennessy, E. J., Sheedy, F. J., Santamaria, D., Barbacid, M., & O'Neill, L. A. J. (2011).  
644 Toll-like receptor-4 (TLR4) down-regulates microRNA-107, increasing macrophage  
645 adhesion via cyclin-dependent kinase 6. *The Journal of Biological Chemistry*,  
646 286(29), 25531–25539. <https://doi.org/10.1074/jbc.M111.256206>
- 647 Hensley, L. E., Fritz, L. E., Jahrling, P. B., Karp, C. L., Huggins, J. W., & Geisbert, T. W.  
648 (2004). Interferon-beta 1a and SARS coronavirus replication. *Emerging Infectious*  
649 *Diseases*, 10(2), 317–319. <https://doi.org/10.3201/eid1002.030482>
- 650 Herreros-Villanueva, M., Zhang, J.-S., Koenig, A., Abel, E. V., Smyrk, T. C., Bamlet, W.  
651 R., de Narvajias, A. A.-M., Gomez, T. S., Simeone, D. M., Bujanda, L., & Billadeau,  
652 D. D. (2013). SOX2 promotes dedifferentiation and imparts stem cell-like features  
653 to pancreatic cancer cells. *Oncogenesis*, 2, e61.  
654 <https://doi.org/10.1038/oncsis.2013.23>
- 655 Hill, C., Jones, M. G., Davies, D. E., & Wang, Y. (2019). Epithelial-mesenchymal  
656 transition contributes to pulmonary fibrosis via aberrant epithelial/fibroblastic cross-  
657 talk. *Journal of Lung Health and Diseases*, 3(2), 31–35.
- 658 Ito, T., Allen, R. M., Carson, W. F. 4th, Schaller, M., Cavassani, K. A., Hogaboam, C.  
659 M., Lukacs, N. W., Matsukawa, A., & Kunkel, S. L. (2011). The critical role of Notch  
660 ligand Delta-like 1 in the pathogenesis of influenza A virus (H1N1) infection. *PLoS*  
661 *Pathogens*, 7(11), e1002341. <https://doi.org/10.1371/journal.ppat.1002341>
- 662 Jiang, R., Li, Y., Xu, Y., Zhou, Y., Pang, Y., Shen, L., Zhao, Y., Zhang, J., Zhou, J.,  
663 Wang, X., & Liu, Q. (2013). EMT and CSC-like properties mediated by the

- 664 IKKbeta/IkappaBalpha/RelA signal pathway via the transcriptional regulator, Snail,  
665 are involved in the arsenite-induced neoplastic transformation of human  
666 keratinocytes. *Archives of Toxicology*, 87(6), 991–1000.  
667 <https://doi.org/10.1007/s00204-012-0933-0>
- 668 Jin, D., & Musier-Forsyth, K. (2019). Role of host tRNAs and aminoacyl-tRNA  
669 synthetases in retroviral replication. *The Journal of Biological Chemistry*, 294(14),  
670 5352–5364. <https://doi.org/10.1074/jbc.REV118.002957>
- 671 Jordan, N. V., Prat, A., Abell, A. N., Zawistowski, J. S., Sciaky, N., Karginova, O. A.,  
672 Zhou, B., Golitz, B. T., Perou, C. M., & Johnson, G. L. (2013). SWI/SNF chromatin-  
673 remodeling factor Smarcd3/Baf60c controls epithelial-mesenchymal transition by  
674 inducing Wnt5a signaling. *Molecular and Cellular Biology*, 33(15), 3011–3025.  
675 <https://doi.org/10.1128/MCB.01443-12>
- 676 Josset, L., Menachery, V. D., Gralinski, L. E., Agnihothram, S., Sova, P., Carter, V. S.,  
677 Yount, B. L., Graham, R. L., Baric, R. S., & Katze, M. G. (2013). Cell host response  
678 to infection with novel human coronavirus EMC predicts potential antivirals and  
679 important differences with SARS coronavirus. *MBio*, 4(3), e00165-13.  
680 <https://doi.org/10.1128/mBio.00165-13>
- 681 Kaldis, P., Ojala, P. M., Tong, L., Makela, T. P., & Solomon, M. J. (2001). CAK-  
682 independent activation of CDK6 by a viral cyclin. *Molecular Biology of the Cell*,  
683 12(12), 3987–3999. <https://doi.org/10.1091/mbc.12.12.3987>
- 684 Kato, N., Kosugi, T., Sato, W., Ishimoto, T., Kojima, H., Sato, Y., Sakamoto, K.,  
685 Maruyama, S., Yuzawa, Y., Matsuo, S., & Kadomatsu, K. (2011). Basigin/CD147  
686 promotes renal fibrosis after unilateral ureteral obstruction. *The American Journal*  
687 *of Pathology*, 178(2), 572–579. <https://doi.org/10.1016/j.ajpath.2010.10.009>
- 688 Klingelhutz, A. J., Foster, S. A., & McDougall, J. K. (1996). Telomerase activation by the  
689 E6 gene product of human papillomavirus type 16. *Nature*, 380(6569), 79–82.  
690 <https://doi.org/10.1038/380079a0>
- 691 Kolosionek, E., Savai, R., Ghofrani, H. A., Weissmann, N., Guenther, A., Grimminger,  
692 F., Seeger, W., Banat, G. A., Schermuly, R. T., & Pullamsetti, S. S. (2009).  
693 Expression and activity of phosphodiesterase isoforms during epithelial  
694 mesenchymal transition: the role of phosphodiesterase 4. *Molecular Biology of the*  
695 *Cell*, 20(22), 4751–4765. <https://doi.org/10.1091/mbc.e09-01-0019>
- 696 Kuo, W.-Y., Wu, C.-Y., Hwu, L., Lee, J.-S., Tsai, C.-H., Lin, K.-P., Wang, H.-E., Chou,  
697 T.-Y., Tsai, C.-M., Gelovani, J., & Liu, R.-S. (2015). Enhancement of tumor initiation  
698 and expression of KCNMA1, MORF4L2 and ASPM genes in the adenocarcinoma  
699 of lung xenograft after vorinostat treatment. *Oncotarget*, 6(11), 8663–8675.  
700 <https://doi.org/10.18632/oncotarget.3536>
- 701 Lamouille, S., Xu, J., & Derynck, R. (2014). Molecular mechanisms of epithelial-  
702 mesenchymal transition. *Nature Reviews. Molecular Cell Biology*, 15(3), 178–196.  
703 <https://doi.org/10.1038/nrm3758>

- 704 Li, H., Zhang, J., Song, X., Wang, T., Li, Z., Hao, D., Wang, X., Zheng, Q., Mao, C., Xu,  
705 P., & Lv, C. (2014). Alveolar epithelial cells undergo epithelial-mesenchymal  
706 transition in acute interstitial pneumonia: a case report. *BMC Pulmonary Medicine*,  
707 14, 67. <https://doi.org/10.1186/1471-2466-14-67>
- 708 Li, N., Gou, J.-H., Xiong, J., You, J.-J., & Li, Z.-Y. (2020). HOXB4 promotes the  
709 malignant progression of ovarian cancer via DHDDS. *BMC Cancer*, 20(1), 222.  
710 <https://doi.org/10.1186/s12885-020-06725-4>
- 711 Liu, T., Zhao, M., Liu, J., He, Z., Zhang, Y., You, H., Huang, J., Lin, X., & Feng, X.-H.  
712 (2017). Tumor suppressor bromodomain-containing protein 7 cooperates with  
713 Smads to promote transforming growth factor-beta responses. *Oncogene*, 36(3),  
714 362–372. <https://doi.org/10.1038/onc.2016.204>
- 715 Liu, X., Fu, Y., Huang, J., Wu, M., Zhang, Z., Xu, R., Zhang, P., Zhao, S., Liu, L., &  
716 Jiang, H. (2019). ADAR1 promotes the epithelial-to-mesenchymal transition and  
717 stem-like cell phenotype of oral cancer by facilitating oncogenic microRNA  
718 maturation. *Journal of Experimental & Clinical Cancer Research : CR*, 38(1), 315.  
719 <https://doi.org/10.1186/s13046-019-1300-2>
- 720 Liu, Y. (2006). Renal fibrosis: new insights into the pathogenesis and therapeutics.  
721 *Kidney International*, 69(2), 213–217. <https://doi.org/10.1038/sj.ki.5000054>
- 722 Liu, Z., Li, Q., Li, K., Chen, L., Li, W., Hou, M., Liu, T., Yang, J., Lindvall, C., Bjorkholm,  
723 M., Jia, J., & Xu, D. (2013). Telomerase reverse transcriptase promotes epithelial-  
724 mesenchymal transition and stem cell-like traits in cancer cells. *Oncogene*, 32(36),  
725 4203–4213. <https://doi.org/10.1038/onc.2012.441>
- 726 Ludwig, S., & Planz, O. (2008). Influenza viruses and the NF-kappaB signaling pathway  
727 - towards a novel concept of antiviral therapy. *Biological Chemistry*, 389(10), 1307–  
728 1312. <https://doi.org/10.1515/BC.2008.148>
- 729 Luo, X., Guo, L., Zhang, J., Xu, Y., Gu, W., Feng, L., & Wang, Y. (2017). Tight Junction  
730 Protein Occludin Is a Porcine Epidemic Diarrhea Virus Entry Factor. *Journal of*  
731 *Virology*, 91(10). <https://doi.org/10.1128/JVI.00202-17>
- 732 Martinelli, P., Carrillo-de Santa Pau, E., Cox, T., Sainz, B. J., Dusetti, N., Greenhalf, W.,  
733 Rinaldi, L., Costello, E., Ghaneh, P., Malats, N., Buchler, M., Pajic, M., Biankin, A.  
734 V, Iovanna, J., Neoptolemos, J., & Real, F. X. (2017). GATA6 regulates EMT and  
735 tumour dissemination, and is a marker of response to adjuvant chemotherapy in  
736 pancreatic cancer. *Gut*, 66(9), 1665–1676. <https://doi.org/10.1136/gutjnl-2015-311256>
- 737
- 738 Mendoza-Rodriguez, M., Arevalo Romero, H., Fuentes-Panana, E. M., Ayala-Summano,  
739 J.-T., & Meza, I. (2017). IL-1beta induces up-regulation of BIRC3, a gene involved  
740 in chemoresistance to doxorubicin in breast cancer cells. *Cancer Letters*, 390, 39–  
741 44. <https://doi.org/10.1016/j.canlet.2017.01.005>
- 742 Ng, S. S. M., Li, A., Pavlakis, G. N., Ozato, K., & Kino, T. (2013). Viral infection

- 743 increases glucocorticoid-induced interleukin-10 production through ERK-mediated  
744 phosphorylation of the glucocorticoid receptor in dendritic cells: potential clinical  
745 implications. *PLoS One*, 8(5), e63587. <https://doi.org/10.1371/journal.pone.0063587>
- 746 Nie, Z., Gao, W., Zhang, Y., Hou, Y., Liu, J., Li, Z., Xue, W., Ye, X., & Jin, A. (2019).  
747 STAG2 loss-of-function mutation induces PD-L1 expression in U2OS cells. *Annals  
748 of Translational Medicine*, 7(7), 127. <https://doi.org/10.21037/atm.2019.02.23>
- 749 Nieto, M. A. (2002). The snail superfamily of zinc-finger transcription factors. *Nature  
750 Reviews. Molecular Cell Biology*, 3(3), 155–166. <https://doi.org/10.1038/nrm757>
- 751 Ochsner, S. A., Abraham, D., Martin, K., Ding, W., McOwiti, A., Kankanamge, W.,  
752 Wang, Z., Andreano, K., Hamilton, R. A., Chen, Y., Hamilton, A., Gantner, M. L.,  
753 Dehart, M., Qu, S., Hilsenbeck, S. G., Becnel, L. B., Bridges, D., Ma'ayan, A.,  
754 Huss, J. M., ... McKenna, N. J. (2019). The Signaling Pathways Project, an  
755 integrated 'omics knowledgebase for mammalian cellular signaling pathways.  
756 *Scientific Data*, 6(1), 252. <https://doi.org/10.1038/s41597-019-0193-4>
- 757 Ostler, J. B., Harrison, K. S., Schroeder, K., Thunuguntla, P., & Jones, C. (2019). The  
758 Glucocorticoid Receptor (GR) Stimulates Herpes Simplex Virus 1 Productive  
759 Infection, in Part Because the Infected Cell Protein 0 (ICP0) Promoter Is  
760 Cooperatively Transactivated by the GR and Kruppel-Like Transcription Factor 15.  
761 *Journal of Virology*, 93(6). <https://doi.org/10.1128/JVI.02063-18>
- 762 Pauls, E., Ruiz, A., Badia, R., Permanyer, M., Gubern, A., Riveira-Munoz, E., Torres-  
763 Torronteras, J., Alvarez, M., Mothe, B., Brander, C., Crespo, M., Menendez-Arias,  
764 L., Clotet, B., Keppler, O. T., Marti, R., Posas, F., Ballana, E., & Este, J. A. (2014).  
765 Cell cycle control and HIV-1 susceptibility are linked by CDK6-dependent CDK2  
766 phosphorylation of SAMHD1 in myeloid and lymphoid cells. *Journal of Immunology  
767 (Baltimore, Md. : 1950)*, 193(4), 1988–1997.  
768 <https://doi.org/10.4049/jimmunol.1400873>
- 769 Perteu, M., Shumate, A., Perteu, G., Varabyou, A., Breitwieser, F. P., Chang, Y.-C.,  
770 Madugundu, A. K., Pandey, A., & Salzberg, S. L. (2018). CHES: a new human  
771 gene catalog curated from thousands of large-scale RNA sequencing experiments  
772 reveals extensive transcriptional noise. *Genome Biology*, 19(1), 208.  
773 <https://doi.org/10.1186/s13059-018-1590-2>
- 774 Poppe, M., Wittig, S., Jurida, L., Bartkuhn, M., Wilhelm, J., Muller, H., Beuerlein, K.,  
775 Karl, N., Bhujju, S., Ziebuhr, J., Schmitz, M. L., & Kracht, M. (2017). The NF-  
776 kappaB-dependent and -independent transcriptome and chromatin landscapes of  
777 human coronavirus 229E-infected cells. *PLoS Pathogens*, 13(3), e1006286.  
778 <https://doi.org/10.1371/journal.ppat.1006286>
- 779 Ruckle, A., Haasbach, E., Julkunen, I., Planz, O., Ehrhardt, C., & Ludwig, S. (2012).  
780 The NS1 protein of influenza A virus blocks RIG-I-mediated activation of the  
781 noncanonical NF-kappaB pathway and p52/RelB-dependent gene expression in  
782 lung epithelial cells. *Journal of Virology*, 86(18), 10211–10217.  
783 <https://doi.org/10.1128/JVI.00323-12>



- 784 Ruster, C., & Wolf, G. (2011). Angiotensin II as a morphogenic cytokine stimulating  
785 renal fibrogenesis. *Journal of the American Society of Nephrology : JASN*, 22(7),  
786 1189–1199. <https://doi.org/10.1681/ASN.2010040384>
- 787 Sahu, S. K., Tiwari, N., Pataskar, A., Zhuang, Y., Borisova, M., Diken, M., Strand, S.,  
788 Beli, P., & Tiwari, V. K. (2017). FBXO32 promotes microenvironment underlying  
789 epithelial-mesenchymal transition via CtBP1 during tumour metastasis and brain  
790 development. *Nature Communications*, 8(1), 1523. <https://doi.org/10.1038/s41467-017-01366-x>  
791
- 792 Sappenfield, E., Jamieson, D. J., & Kourtis, A. P. (2013). Pregnancy and susceptibility  
793 to infectious diseases. *Infectious Diseases in Obstetrics and Gynecology*, 2013,  
794 752852. <https://doi.org/10.1155/2013/752852>
- 795 Schneider, W. M., Chevillotte, M. D., & Rice, C. M. (2014). Interferon-stimulated genes:  
796 a complex web of host defenses. *Annual Review of Immunology*, 32, 513–545.  
797 <https://doi.org/10.1146/annurev-immunol-032713-120231>
- 798 Schulze-Gahmen, U., Upton, H., Birnberg, A., Bao, K., Chou, S., Krogan, N. J., Zhou,  
799 Q., & Alber, T. (2013). The AFF4 scaffold binds human P-TEFb adjacent to HIV  
800 Tat. *ELife*, 2, e00327. <https://doi.org/10.7554/eLife.00327>
- 801 Sims, A. C., Tilton, S. C., Menachery, V. D., Gralinski, L. E., Schafer, A., Matzke, M. M.,  
802 Webb-Robertson, B.-J. M., Chang, J., Luna, M. L., Long, C. E., Shukla, A. K.,  
803 Bankhead, A. R. 3rd, Burkett, S. E., Zornetzer, G., Tseng, C.-T. K., Metz, T. O.,  
804 Pickles, R., McWeeney, S., Smith, R. D., ... Baric, R. S. (2013). Release of severe  
805 acute respiratory syndrome coronavirus nuclear import block enhances host  
806 transcription in human lung cells. *Journal of Virology*, 87(7), 3885–3902.  
807 <https://doi.org/10.1128/JVI.02520-12>
- 808 Siraj, A. K., Pratheeshkumar, P., Divya, S. P., Parvathareddy, S. K., Bu, R., Masoodi,  
809 T., Kong, Y., Thangavel, S., Al-Sanea, N., Ashari, L. H., Abduljabbar, A., Al-  
810 Homoud, S., Al-Dayel, F., & Al-Kuraya, K. S. (2019). TGFbeta-induced SMAD4-  
811 dependent Apoptosis Proceeded by EMT in CRC. *Molecular Cancer Therapeutics*,  
812 18(7), 1312–1322. <https://doi.org/10.1158/1535-7163.MCT-18-1378>
- 813 Siston, A. M., Rasmussen, S. A., Honein, M. A., Fry, A. M., Seib, K., Callaghan, W. M.,  
814 Louie, J., Doyle, T. J., Crockett, M., Lynfield, R., Moore, Z., Wiedeman, C., Anand,  
815 M., Tabony, L., Nielsen, C. F., Waller, K., Page, S., Thompson, J. M., Avery, C., ...  
816 Jamieson, D. J. (2010). Pandemic 2009 influenza A(H1N1) virus illness among  
817 pregnant women in the United States. *JAMA*, 303(15), 1517–1525.  
818 <https://doi.org/10.1001/jama.2010.479>
- 819 Stark, G. R., Kerr, I. M., Williams, B. R., Silverman, R. H., & Schreiber, R. D. (1998).  
820 How cells respond to interferons. *Annual Review of Biochemistry*, 67, 227–264.  
821 <https://doi.org/10.1146/annurev.biochem.67.1.227>
- 822 Subramanian, A., Tamayo, P., Mootha, V. K., Mukherjee, S., Ebert, B. L., Gillette, M. A.,  
823 Paulovich, A., Pomeroy, S. L., Golub, T. R., Lander, E. S., & Mesirov, J. P. (2005).

- 824 Gene set enrichment analysis: a knowledge-based approach for interpreting  
825 genome-wide expression profiles. *Proceedings of the National Academy of*  
826 *Sciences of the United States of America*, 102(43), 15545–15550.  
827 <https://doi.org/10.1073/pnas.0506580102>
- 828 Suh, Y., Yoon, C.-H., Kim, R.-K., Lim, E.-J., Oh, Y. S., Hwang, S.-G., An, S., Yoon, G.,  
829 Gye, M. C., Yi, J.-M., Kim, M.-J., & Lee, S.-J. (2013). Claudin-1 induces epithelial-  
830 mesenchymal transition through activation of the c-Abl-ERK signaling pathway in  
831 human liver cells. *Oncogene*, 32(41), 4873–4882.  
832 <https://doi.org/10.1038/onc.2012.505>
- 833 Takahashi, K., Halfmann, P., Oyama, M., Kozuka-Hata, H., Noda, T., & Kawaoka, Y.  
834 (2013). DNA topoisomerase 1 facilitates the transcription and replication of the  
835 Ebola virus genome. *Journal of Virology*, 87(16), 8862–8869.  
836 <https://doi.org/10.1128/JVI.03544-12>
- 837 Takeda, K., Kaisho, T., & Akira, S. (2003). Toll-like receptors. *Annual Review of*  
838 *Immunology*, 21, 335–376.  
839 <https://doi.org/10.1146/annurev.immunol.21.120601.141126>
- 840 Taki, M., Abiko, K., Baba, T., Hamanishi, J., Yamaguchi, K., Murakami, R., Yamanoi, K.,  
841 Horikawa, N., Hosoe, Y., Nakamura, E., Sugiyama, A., Mandai, M., Konishi, I., &  
842 Matsumura, N. (2018). Snail promotes ovarian cancer progression by recruiting  
843 myeloid-derived suppressor cells via CXCR2 ligand upregulation. *Nature*  
844 *Communications*, 9(1), 1685. <https://doi.org/10.1038/s41467-018-03966-7>
- 845 Tecalco-Cruz, A. C., Rios-Lopez, D. G., Vazquez-Victorio, G., Rosales-Alvarez, R. E., &  
846 Macias-Silva, M. (2018). Transcriptional cofactors Ski and SnoN are major  
847 regulators of the TGF-beta/Smad signaling pathway in health and disease. *Signal*  
848 *Transduction and Targeted Therapy*, 3, 15. [https://doi.org/10.1038/s41392-018-](https://doi.org/10.1038/s41392-018-0015-8)  
849 [0015-8](https://doi.org/10.1038/s41392-018-0015-8)
- 850 Totura, A. L., & Bavari, S. (2019). Broad-spectrum coronavirus antiviral drug discovery.  
851 *Expert Opinion on Drug Discovery*, 14(4), 397–412.  
852 <https://doi.org/10.1080/17460441.2019.1581171>
- 853 Totura, A. L., Whitmore, A., Agnihothram, S., Schafer, A., Katze, M. G., Heise, M. T., &  
854 Baric, R. S. (2015). Toll-Like Receptor 3 Signaling via TRIF Contributes to a  
855 Protective Innate Immune Response to Severe Acute Respiratory Syndrome  
856 Coronavirus Infection. *MBio*, 6(3), e00638-15. [https://doi.org/10.1128/mBio.00638-](https://doi.org/10.1128/mBio.00638-15)  
857 [15](https://doi.org/10.1128/mBio.00638-15)
- 858 Vukmirovic, M., Herazo-Maya, J. D., Blackmon, J., Skodric-Trifunovic, V., Jovanovic, D.,  
859 Pavlovic, S., Stojic, J., Zeljkovic, V., Yan, X., Homer, R., Stefanovic, B., &  
860 Kaminski, N. (2017). Identification and validation of differentially expressed  
861 transcripts by RNA-sequencing of formalin-fixed, paraffin-embedded (FFPE) lung  
862 tissue from patients with Idiopathic Pulmonary Fibrosis. *BMC Pulmonary Medicine*,  
863 17(1), 15. <https://doi.org/10.1186/s12890-016-0356-4>

- 864 Wan, L. C. K., Maisonneuve, P., Szilard, R. K., Lambert, J.-P., Ng, T. F., Manczyk, N.,  
865 Huang, H., Laister, R., Caudy, A. A., Gingras, A.-C., Durocher, D., & Sicheri, F.  
866 (2017). Proteomic analysis of the human KEOPS complex identifies C14ORF142  
867 as a core subunit homologous to yeast Gon7. *Nucleic Acids Research*, *45*(2), 805–  
868 817. <https://doi.org/10.1093/nar/gkw1181>
- 869 Wang, C.-A., Drasin, D., Pham, C., Jedlicka, P., Zaberezhnyy, V., Guney, M., Li, H.,  
870 Nemenoff, R., Costello, J. C., Tan, A.-C., & Ford, H. L. (2014). Homeoprotein Six2  
871 promotes breast cancer metastasis via transcriptional and epigenetic control of E-  
872 cadherin expression. *Cancer Research*, *74*(24), 7357–7370.  
873 <https://doi.org/10.1158/0008-5472.CAN-14-0666>
- 874 Wang, C., Zhang, J., Fok, K. L., Tsang, L. L., Ye, M., Liu, J., Li, F., Zhao, A. Z., Chan,  
875 H. C., & Chen, H. (2018). CD147 Induces Epithelial-to-Mesenchymal Transition by  
876 Disassembling Cellular Apoptosis Susceptibility Protein/E-Cadherin/beta-Catenin  
877 Complex in Human Endometriosis. *The American Journal of Pathology*, *188*(7),  
878 1597–1607. <https://doi.org/10.1016/j.ajpath.2018.03.004>
- 879 Wang, K., & Li, J. (2016). Overexpression of ANXA3 is an independent prognostic  
880 indicator in gastric cancer and its depletion suppresses cell proliferation and tumor  
881 growth. *Oncotarget*, *7*(52), 86972–86984.  
882 <https://doi.org/10.18632/oncotarget.13493>
- 883 Wang, S., Lei, T., Zhang, K., Zhao, W., Fang, L., Lai, B., Han, J., Xiao, L., & Wang, N.  
884 (2014). Xenobiotic pregnane X receptor (PXR) regulates innate immunity via  
885 activation of NLRP3 inflammasome in vascular endothelial cells. *The Journal of*  
886 *Biological Chemistry*, *289*(43), 30075–30081.  
887 <https://doi.org/10.1074/jbc.M114.578781>
- 888 Wang, W., Ye, L., Ye, L., Li, B., Gao, B., Zeng, Y., Kong, L., Fang, X., Zheng, H., Wu,  
889 Z., & She, Y. (2007). Up-regulation of IL-6 and TNF-alpha induced by SARS-  
890 coronavirus spike protein in murine macrophages via NF-kappaB pathway. *Virus*  
891 *Research*, *128*(1–2), 1–8. <https://doi.org/10.1016/j.virusres.2007.02.007>
- 892 Wei, C.-Y., Zhu, M.-X., Yang, Y.-W., Zhang, P.-F., Yang, X., Peng, R., Gao, C., Lu, J.-  
893 C., Wang, L., Deng, X.-Y., Lu, N.-H., Qi, F.-Z., & Gu, J.-Y. (2019). Downregulation  
894 of RNF128 activates Wnt/beta-catenin signaling to induce cellular EMT and  
895 stemness via CD44 and CTTN ubiquitination in melanoma. *Journal of Hematology*  
896 *& Oncology*, *12*(1), 21. <https://doi.org/10.1186/s13045-019-0711-z>
- 897 Wobbe, C. R., Dean, F. B., Murakami, Y., Borowiec, J. A., Bullock, P., & Hurwitz, J.  
898 (1987). In vitro replication of DNA containing either the SV40 or the polyoma origin.  
899 *Philosophical Transactions of the Royal Society of London. Series B, Biological*  
900 *Sciences*, *317*(1187), 439–453. <https://doi.org/10.1098/rstb.1987.0071>
- 901 Xia, L., Dai, L., Yu, Q., & Yang, Q. (2017). Persistent Transmissible Gastroenteritis  
902 Virus Infection Enhances Enterotoxigenic Escherichia coli K88 Adhesion by  
903 Promoting Epithelial-Mesenchymal Transition in Intestinal Epithelial Cells. *Journal*  
904 *of Virology*, *91*(21). <https://doi.org/10.1128/JVI.01256-17>

- 905 Xu, C.-B., Liu, X.-S.-B.-J., Li, J.-Q., Zhao, X., Xin, D., & Yu, D. (2019). microRNA-539  
906 functions as a tumor suppressor in papillary thyroid carcinoma via the transforming  
907 growth factor beta1/Smads signaling pathway by targeting secretory leukocyte  
908 protease inhibitor. *Journal of Cellular Biochemistry*, 120(6), 10830–10846.  
909 <https://doi.org/10.1002/jcb.28374>
- 910 Yamajuku, D., Shibata, Y., Kitazawa, M., Katakura, T., Urata, H., Kojima, T., Nakata, O.,  
911 & Hashimoto, S. (2010). Identification of functional clock-controlled elements  
912 involved in differential timing of Per1 and Per2 transcription. *Nucleic Acids  
913 Research*, 38(22), 7964–7973. <https://doi.org/10.1093/nar/gkq678>
- 914 Yang, J., Deng, X., Deng, L., Gu, H., Fan, W., & Cao, Y. (2004). Telomerase activation  
915 by Epstein-Barr virus latent membrane protein 1 is associated with c-Myc  
916 expression in human nasopharyngeal epithelial cells. *Journal of Experimental &  
917 Clinical Cancer Research : CR*, 23(3), 495–506.
- 918 Yin, L., Hubbard, A. K., & Giardina, C. (2000). NF-kappa B regulates transcription of the  
919 mouse telomerase catalytic subunit. *The Journal of Biological Chemistry*, 275(47),  
920 36671–36675. <https://doi.org/10.1074/jbc.M007378200>
- 921 Yoshikawa, T., Hill, T. E., Yoshikawa, N., Popov, V. L., Galindo, C. L., Garner, H. R.,  
922 Peters, C. J., & Tseng, C.-T. K. (2010). Dynamic innate immune responses of  
923 human bronchial epithelial cells to severe acute respiratory syndrome-associated  
924 coronavirus infection. *PloS One*, 5(1), e8729.  
925 <https://doi.org/10.1371/journal.pone.0008729>
- 926 Zaborowska, J., Isa, N. F., & Murphy, S. (2016). P-TEFb goes viral. *BioEssays : News  
927 and Reviews in Molecular, Cellular and Developmental Biology*, 38 Suppl 1, S75-  
928 85. <https://doi.org/10.1002/bies.201670912>
- 929 Zhang, L., Wang, X., Lai, C., Zhang, H., & Lai, M. (2019). PMEPA1 induces EMT via a  
930 non-canonical TGF-beta signalling in colorectal cancer. *Journal of Cellular and  
931 Molecular Medicine*, 23(5), 3603–3615. <https://doi.org/10.1111/jcmm.14261>
- 932 Zhao, M., Kong, L., Liu, Y., & Qu, H. (2015). dbEMT: an epithelial-mesenchymal  
933 transition associated gene resource. *Scientific Reports*, 5, 11459.  
934 <https://doi.org/10.1038/srep11459>
- 935 Zheng, K., Kitazato, K., & Wang, Y. (2014). Viruses exploit the function of epidermal  
936 growth factor receptor. *Reviews in Medical Virology*, 24(4), 274–286.  
937 <https://doi.org/10.1002/rmv.1796>
- 938 Zhou, F., Geng, J., Xu, S., Meng, Q., Chen, K., Liu, F., Yang, F., Pan, B., & Yu, Y.  
939 (2019). FAM83A signaling induces epithelial-mesenchymal transition by the  
940 PI3K/AKT/Snail pathway in NSCLC. *Aging*, 11(16), 6069–6088.  
941 <https://doi.org/10.18632/aging.102163>
- 942 Zhou, P., Yang, X.-L., Wang, X.-G., Hu, B., Zhang, L., Zhang, W., Si, H.-R., Zhu, Y., Li,  
943 B., Huang, C.-L., Chen, H.-D., Chen, J., Luo, Y., Guo, H., Jiang, R.-D., Liu, M.-Q.,

944           Chen, Y., Shen, X.-R., Wang, X., ... Shi, Z.-L. (2020). A pneumonia outbreak  
945           associated with a new coronavirus of probable bat origin. *Nature*, 579(7798), 270–  
946           273. <https://doi.org/10.1038/s41586-020-2012-7>

947



949 **Figure Titles Legends**

950 **Figure 1. Ranking of ISGs in the human ALL CoV infection transcriptomic**

951 **consensome.** See Supplementary information, Section 2, column I.

952 **Figure 2. GeneOverlap analysis of CoV and IAV TC95s and SPP receptor or**

953 **enzyme TC95s.** OR: Odds ratio. All ORs are  $p < 0.05$ . Numerical data are provided in

954 Supplementary information Section 8.

955 **Figure 3. GeneOverlap analysis of CoV and IAV TC95s and ChIP-Atlas**

956 **transcription factor CC95s.** OR: Odds ratio. All ORs are  $p < 0.05$ . Numerical data are

957 provided in Supplementary information Section 8.

958 **Figure 4. GeneOverlap analysis of CoV and IAV TC95s and ChIP-Atlas enzyme**

959 **CC95s.** OR: Odds ratio. Numerical data are provided in Supplementary information

960 Section 8. All ORs are  $p < 0.05$ .

961 **Figure 5. GeneOverlap analysis of CoV and IAV TC95s and ChIP-Atlas co-node**

962 **CC95s.** OR: Odds ratio. Numerical data are provided in Supplementary information

963 Section 8. All ORs are  $p < 0.05$ .

964 **Figure 6. Antagonism between PGR and IFNR signaling in the regulation of viral**

965 **response genes in the airway epithelium.** PGR loss of function experiments were

966 retrieved from GSE17307 (SPP DOI 10.1621/xigKzGn1se).

967 **Figure 7. Conservation of polarity of differential expression in CoV, IFNR and**

968 **TERT perturbation transcriptomic experiments across diverse canonical**

969 **interferon-inducible viral response genes.** Positive/negative regulatory relationship

970 of TERT with a transcriptional target was inferred from the design of the underlying

971 experiments: this was loss of function for experiments in GSE77014 (MST132 inhibitor)  
972 and GSE60175 (shRNA), and gain of function in E-MEXP-563 (overexpression). All  
973 IFNR experiments were gain of function using characterized physiological ligands for  
974 members of the family.

975 **Figure 8. Identification of a SARS2 epithelial to mesenchymal transcriptional**  
976 **signature.** Note that the SARS2 genes are all in the 99<sup>th</sup> percentile and are therefore  
977 superimposed in the scatterplot. Indicated are the results of the Paired Two Sample for  
978 Means t-Test comparing the Relative Ranks of the genes in the SARS2 consensome  
979 with those in the SARS1, MERS and IAV consensomes.

980



981 **Tables**

982 **Table 1. Genes in the 99<sup>th</sup> %ile of the ALL CoV consensome and the 50<sup>th</sup>**  
983 **percentile of the IAV consensome**

<b>Symbol</b>	<b>Name</b>	<b>CONSENSOME %ILE</b>	
		<b>All CoV</b>	<b>IAV</b>
<i>GEM</i>	GTP binding protein overexpressed in skeletal muscle	99	43
<i>DHRS1</i>	dehydrogenase/reductase 1	99	43
<i>NIPSNAP3A</i>	nipsnap homolog 3A	99	43
<i>SFSWAP</i>	splicing factor SWAP	99	43
<i>GON7</i>	GON7 subunit of KEOPS complex	99	39
<i>INHBA</i>	inhibin subunit beta A	99	37
<i>PDZK1</i>	PDZ domain containing 1	99	37
<i>PER1</i>	period circadian regulator 1	99	33
<i>PAQR6</i>	progesterin and adipoQ receptor family member 6	99	33
<i>IFT20</i>	intraflagellar transport 20	99	33
<i>ZNF628</i>	zinc finger protein 628	99	33
<i>KANSL1</i>	KAT8 regulatory NSL complex subunit 1	99	33
<i>CREB5</i>	cAMP responsive element binding protein 5	99	27
<i>PER2</i>	period circadian regulator 2	99	17
<i>TJAP1</i>	tight junction associated protein 1	99	17

984

985

986

987 **Table 2. Links to SPP Regulation Reports for the top 20 ranked genes in the ALL**

988 **CoV consensome**

<b>Symbol</b>	<b>Name</b>	<b>Link</b>
<i>JUN</i>	Jun proto-oncogene, AP-1 transcription factor subunit	<a href="#">SPP Regulation Report</a>
<i>DUSP1</i>	dual specificity phosphatase 1	<a href="#">SPP Regulation Report</a>
<i>FOS</i>	Fos proto-oncogene, AP-1 transcription factor subunit	<a href="#">SPP Regulation Report</a>
<i>EGR1</i>	early growth response 1	<a href="#">SPP Regulation Report</a>
<i>CXCL2</i>	C-X-C motif chemokine ligand 2	<a href="#">SPP Regulation Report</a>
<i>TNFAIP3</i>	TNF alpha induced protein 3	<a href="#">SPP Regulation Report</a>
<i>IER2</i>	immediate early response 2	<a href="#">SPP Regulation Report</a>
<i>CCNL1</i>	cyclin L1	<a href="#">SPP Regulation Report</a>
<i>PIM3</i>	Pim-3 proto-oncogene, serine/threonine kinase	<a href="#">SPP Regulation Report</a>
<i>CSRNP1</i>	cysteine and serine rich nuclear protein 1	<a href="#">SPP Regulation Report</a>
<i>FOSB</i>	FosB proto-oncogene, AP-1 transcription factor subunit	<a href="#">SPP Regulation Report</a>
<i>ZC3H12A</i>	zinc finger CCCH-type containing 12A	<a href="#">SPP Regulation Report</a>
<i>ZFP36</i>	ZFP36 ring finger protein	<a href="#">SPP Regulation Report</a>
<i>BHLHE40</i>	basic helix-loop-helix family member e40	<a href="#">SPP Regulation Report</a>
<i>RELB</i>	RELB proto-oncogene, NF-kB subunit	<a href="#">SPP Regulation Report</a>
<i>EGR2</i>	early growth response 2	<a href="#">SPP Regulation Report</a>
<i>NFKBIA</i>	NFKB inhibitor alpha	<a href="#">SPP Regulation Report</a>
<i>BCL3</i>	BCL3 transcription coactivator	<a href="#">SPP Regulation Report</a>
<i>YRDC</i>	yrdC N6-threonylcarbamoyltransferase domain containing	<a href="#">SPP Regulation Report</a>
<i>IFIT1</i>	interferon induced protein with tetratricopeptide repeats 1	<a href="#">SPP Regulation Report</a>

989

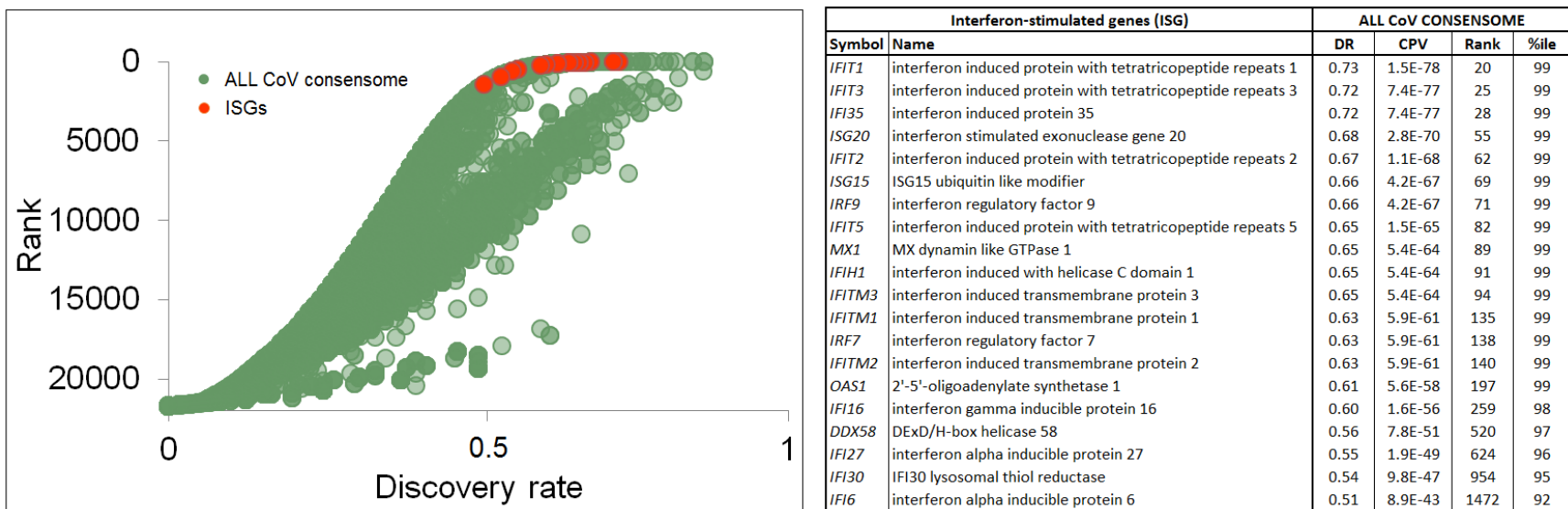


Figure 1

Figure 2

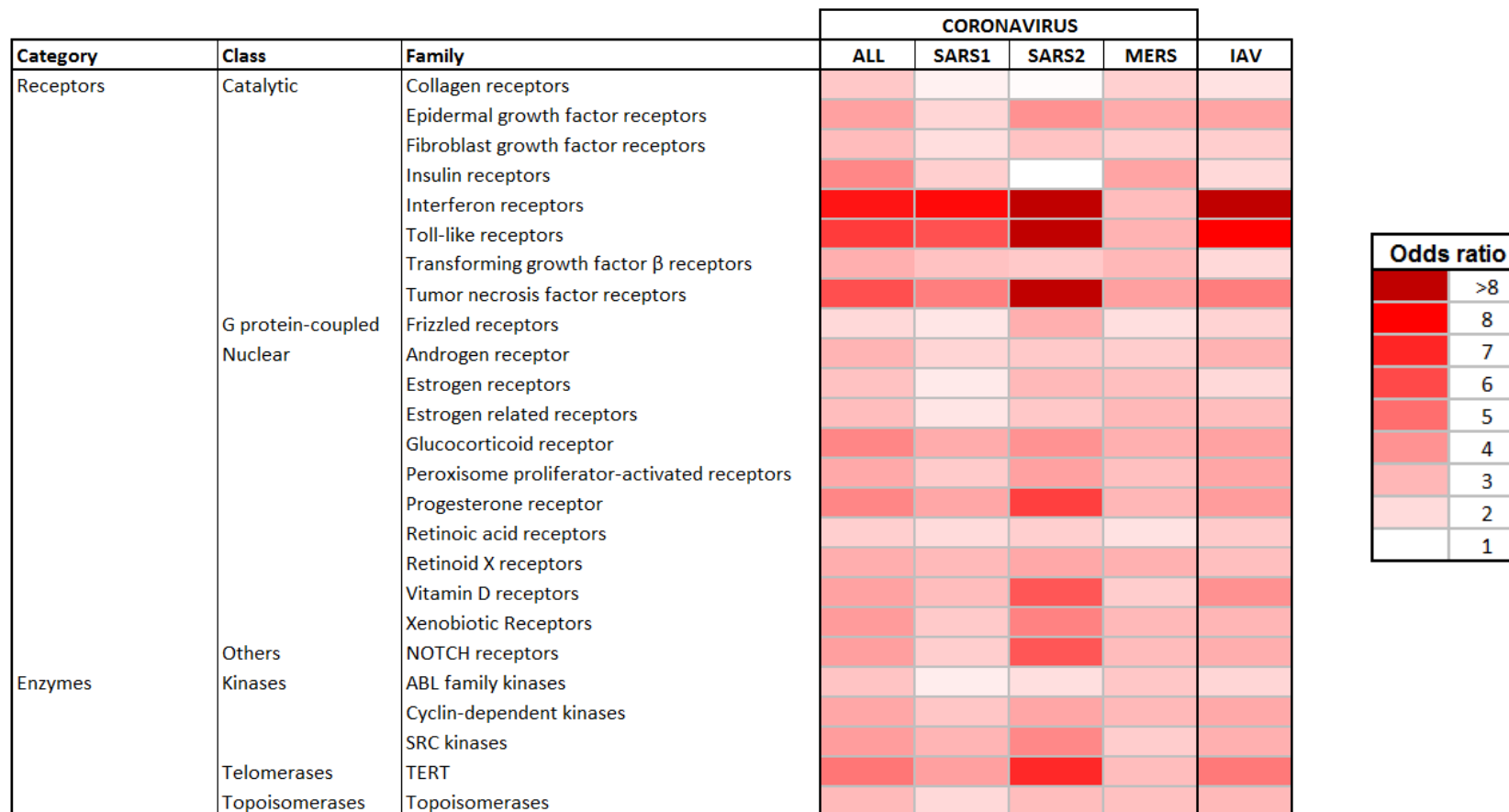




Figure 3

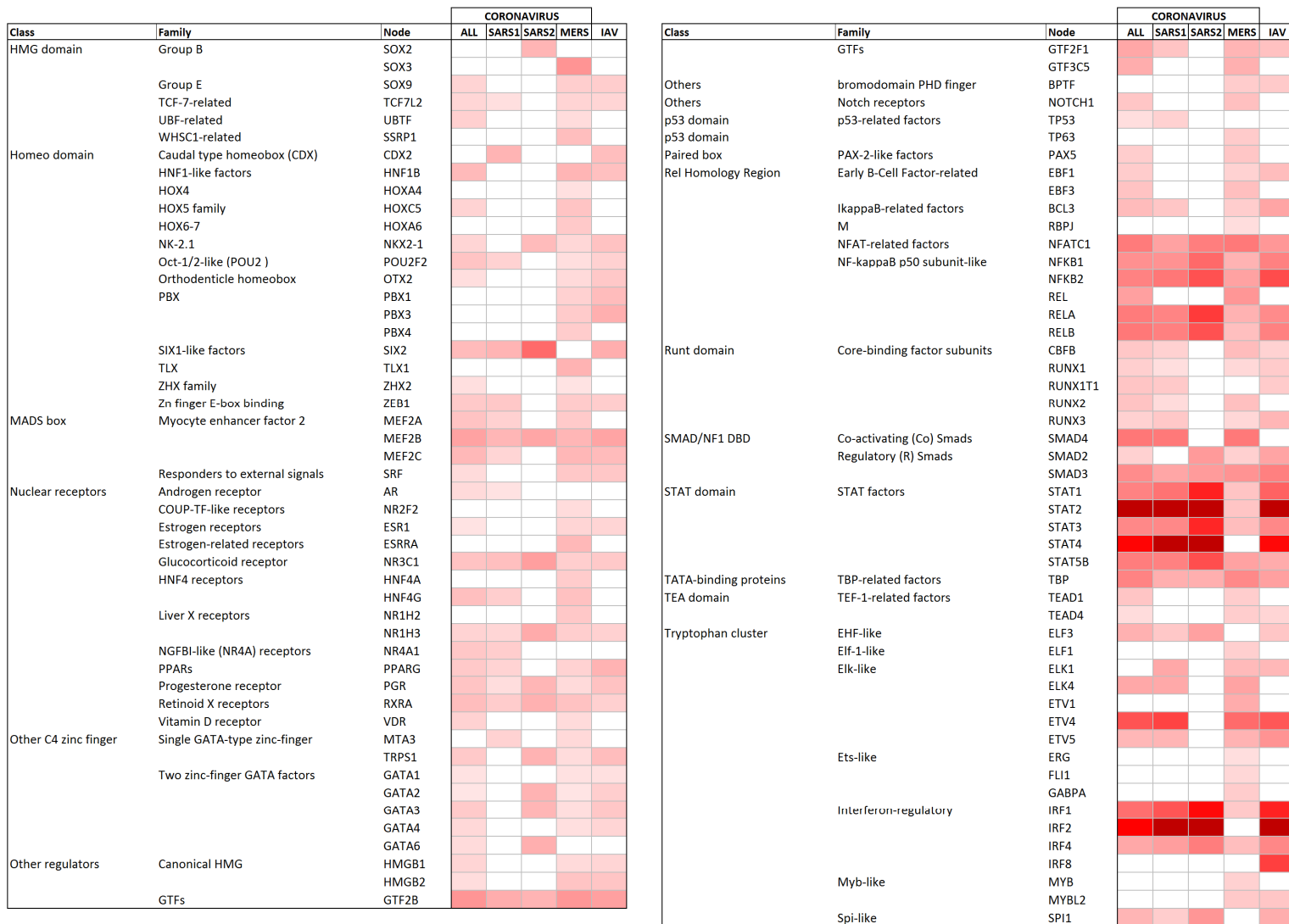


Figure 3 (contd)

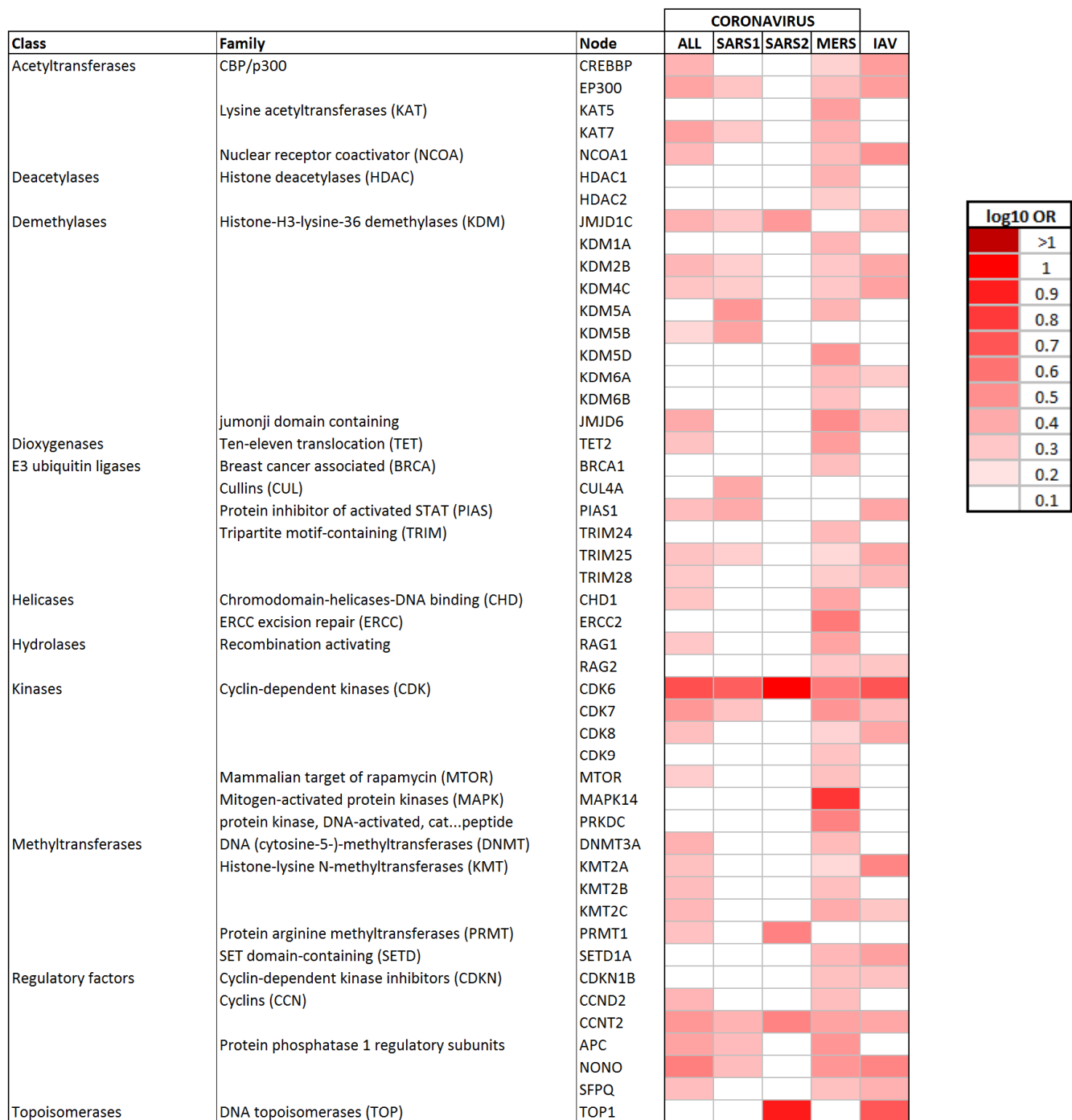


Figure 4

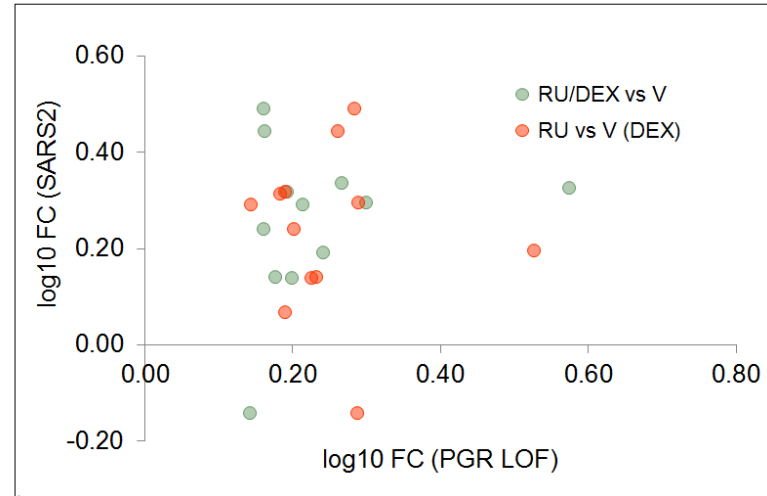


Figure 5



Figure 6

Symbol	Name	log10 FC SARS2	log10 FC PGR loss of function	
			RU/DEX vs V	RU vs V (DEX)
<i>CXCL2</i>	C-X-C motif chemokine ligand 2	0.33	0.57	
<i>IL1B</i>	interleukin 1 beta	0.30	0.30	0.29
<i>TNFAIP3</i>	TNF alpha induced protein 3	0.34	0.27	
<i>NFKBIA</i>	NFKB inhibitor alpha	0.19	0.24	
<i>ISG15</i>	ISG15 ubiquitin like modifier	0.88	0.23	0.27
<i>STAT1</i>	signal transducer and activator of transcription 1	0.29	0.21	0.14
<i>ISG20</i>	interferon stimulated exonuclease gene 20	0.14	0.20	0.22
<i>IFI35</i>	interferon induced protein 35	0.32	0.19	0.19
<i>IFITM2</i>	interferon induced transmembrane protein 2	0.14	0.18	0.23
<i>IFIT3</i>	interferon induced protein with tetratricopeptide repeats	0.45	0.16	0.26
<i>OAS1</i>	2'-5'-oligoadenylate synthetase 1	0.49	0.16	0.28
<i>IFITM3</i>	interferon induced transmembrane protein 3	0.24	0.16	0.20
<i>CXXC5</i>	CXXC finger protein 5	-0.14	0.14	0.29
<i>IER3</i>	immediate early response 3	0.20		0.53
<i>MYD88</i>	MYD88 innate immune signal transduction adaptor	0.07		0.19
<i>CXCL1</i>	C-X-C motif chemokine ligand 1	0.32		0.18



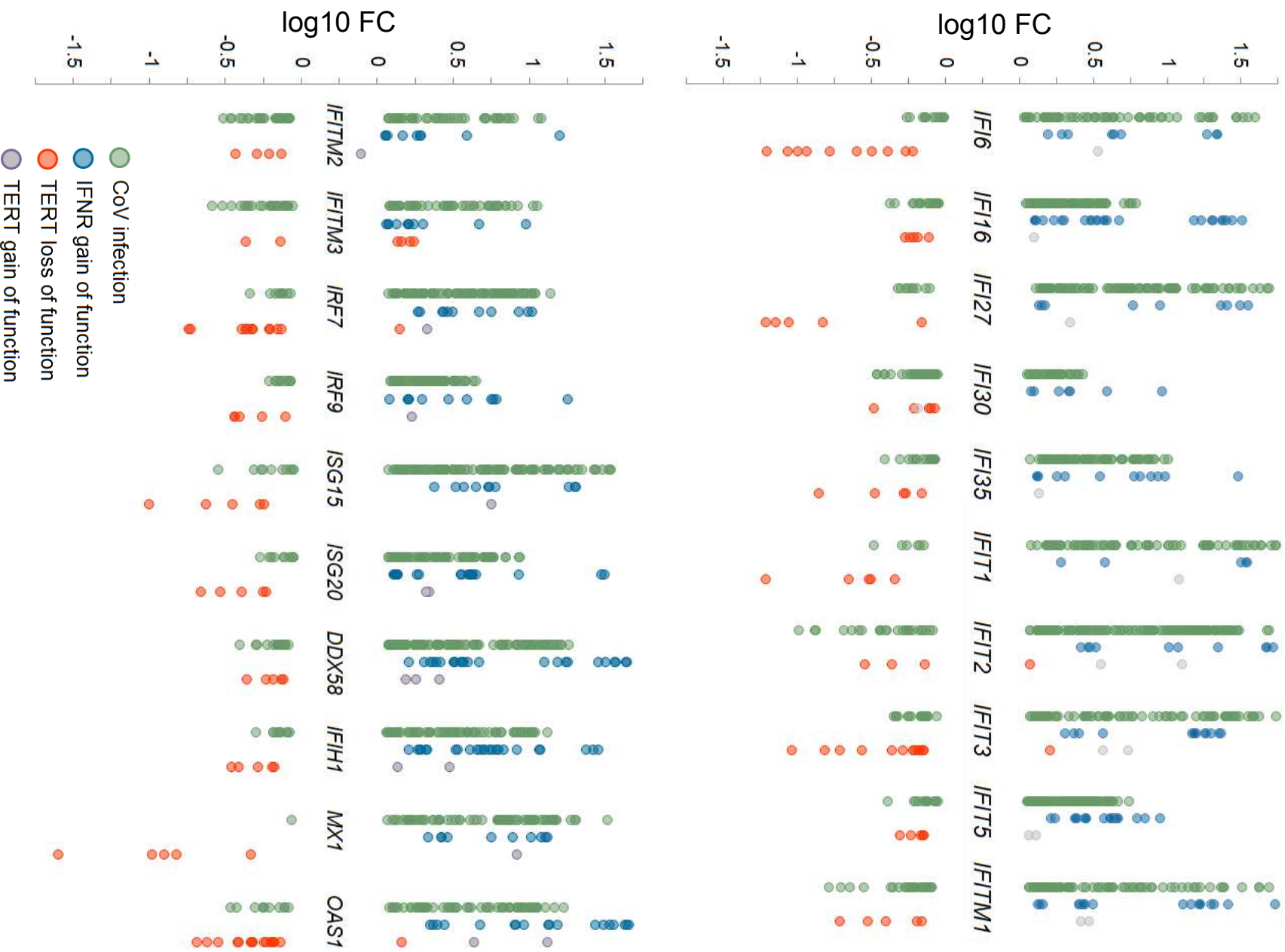


Figure 7

Figure 8

EPITHELIAL TO MESENCHYMAL TRANSITION (EMT) GENES		CONSENSOME %ILE				EMT REFERENCE
Symbol	Name	SARS2	SARS1	MERS	IAV	
<i>ADAR</i>	adenosine deaminase RNA specific	99	96	43	98	Liu et al., 2019
<i>ANXA3</i>	annexin A3	99	80	86	43	Wang & Li, 2016
<i>BIRC3</i>	baculoviral IAP repeat containing 3	99	98	96	94	Mendoza et al., 2017
<i>CLDN1</i>	claudin 1	99	47	83	97	Suh et al., 2013
<i>CXCL2</i>	C-X-C motif chemokine ligand 2	99	99	99	99	Taki et al., 2018
<i>DHDDS</i>	dehydrodolichyl diphosphate synthase subunit	99	23	49	43	Li et al., 2020
<i>FAM83A</i>	family with sequence similarity 83 member A	99	31	3	47	Zhou et al., 2019
<i>IRF9</i>	interferon regulatory factor 9	99	99	91	99	Doherty et al., 2017
<i>KCNMA1</i>	potassium calcium-activated channel subfamily M alpha	99	10	2	10	Kuo et al., 2015
<i>PDE4B</i>	phosphodiesterase 4B	99	61	99	82	Kolosionek et al., 2009
<i>RNF128</i>	ring finger protein 128	99	84	60	86	Wei et al., 2019
<i>RRAGD</i>	Ras related GTP binding D	99	76	79	94	Jordan et al., 2013
<i>SOD2</i>	superoxide dismutase 2	99	84	91	97	Chang et al., 2016

